

# Comparative anatomy of otomorphan epibranchial organs

Allyson J. Evans<sup>1</sup>  | Joshua P. Egan<sup>2</sup> | Jonathan M. Huie<sup>1</sup> |  
L. Patricia Hernandez<sup>1</sup> 

<sup>1</sup>Department of Biological Sciences, The George Washington University, Washington, DC, USA

<sup>2</sup>Bell Museum of Natural History, University of Minnesota, Saint Paul, Minnesota, USA

## Correspondence

Allyson J. Evans, Department of Biological Sciences, The George Washington University, Washington, DC, USA.  
Email: [allysonevans@gwmail.gwu.edu](mailto:allysonevans@gwmail.gwu.edu)

## Funding information

George Washington University Wilbur V. Harlan Research Fellowship; National Science Foundation, Grant/Award Number: DGE-1746914

## Abstract

Certain microphagous fishes possess an epibranchial organ (EBO), a paired muscular pocket-like structure in the posterior pharynx, that facilitates the aggregation of small food items entering the oropharyngeal cavity. Morphologically complex and phylogenetically diverse, the anatomy of EBOs has been described in a small number of taxa that possess this structure, in many cases without a thorough investigation at the microscopic and ultrastructural level. Additionally, the evolution of EBOs has not been rigorously examined within a phylogenetic comparative context, leaving many unanswered questions about how the morphological diversity of EBOs relates to historical patterns and ecology. We characterized the anatomy, histological architecture, and structural patterns of EBOs in 13 otomorphan species belonging to the orders Clupeiformes, Gonorynchiformes, and Characiformes; this sampling includes *Cetengraulis edentulus*, *Nematalosa come*, and *Tenualosa thibaudeaui*, in which the presence of an EBO has not been previously documented. We then conducted a preliminary investigation of relationships between otomorphan EBO anatomy, phylogeny, and diet. Patterns of anatomical diversity were best explained by variation along five morphological axes: shape, size, associated gill rakers, muscularity, and adiposity. EBOs consisted of bilaterally paired diverticula surrounded by layers of circumferential and longitudinal muscle and varying amounts of adipose tissue. Papillae were found in the epithelium lining the diverticulum of each organ; they varied in length and width along the proximodistal axis of the diverticulum and were studded with mucus-producing cells. We found that EBO anatomy was not strongly correlated with phylogenetic relatedness but was moderately correlated with diet in some instances. We hypothesize that EBOs have independently evolved in Otomorpha multiple times via a conserved developmental pathway that makes use of the same underlying tissue types to construct morphologically diverse structures. These findings suggest that there are multiple ways to build an EBO using the same basic anatomical components to achieve the same functional goal—the aggregation of small prey.

## KEY WORDS

epibranchial organ, fish feeding, microphagy, particulate feeding, posterior pharynx

## 1 | INTRODUCTION

As the most speciose and morphologically diverse group of vertebrates, fishes have unsurprisingly amassed an extensive and active body of anatomical research. A cursory survey of recent literature will reveal that a substantial amount of this research is focused on structures related to feeding, such as the oral jaws, teeth, and the muscles that effect movement of the mouth—structures that are for the most part located at the anterior end of the head and pharynx (Camp et al., 2015; Heiple et al., 2023; Huie et al., 2020; Hundt et al., 2014; Hundt & Simons, 2018; Kolmann et al., 2018; Kolmann et al., 2021). With the exception of the pharyngeal jaws, many structures of the posterior pharynx have largely been ignored since their original descriptions (Pos et al., 2019; Roberts-Hughes et al., 2024). While invaluable, these purely anatomical treatments lack the informative power afforded by functional and comparative analyses, which shed light on evolutionary patterns, developmental histories, and the ecological demands faced by related organisms throughout their morphological diversification. In teleost fishes, examples of pharyngeal structures associated with feeding include but are not limited to the pharyngobranchial organ, the epibranchial lobe, and the palatal organ (Brodnick et al., 2022; Capanna et al., 1974; Dosey & Bart Jr., 2011; Weller et al., 2017), many of which are found in microphagous species (those feeding on food items too small to be sensed and consumed individually (Jørgensen, 1966; Sanderson & Wassersug, 1993)).

The ability to extract small food items from large volumes of water is widespread among microphagous fishes, all of which face the same metabolic hurdle of consuming sufficient quantities of minute, edible particles to meet their nutritional needs (Durbin et al., 1981; Pandian & Vivekanandan, 1985; Sims, 2000). Much of the existing research on feeding in microphagous fishes is concerned with the process of prey extraction from particle-laden water, a process facilitated by the gill rakers, which bear a length, shape, spacing, and ultrastructure specific to the species' feeding ecology and filtration mechanism (Almeida et al., 2013; Friedland, 1985; Kahane-Rapport & Paig-Tran, 2024; Paig-Tran & Summers, 2014; Sanderson, 2024; Sanderson et al., 2001). There is, however, another component of feeding on small prey that merits further study: the secondary aggregation of captured food particles following filtration and prior to ingestion. In many species of bony fishes, this aggregation is thought to be accomplished by epibranchial organs: bilaterally paired, muscular pouch-like structures that are supported by the dorsal elements of the posterior gill arches (Figure 1) (Bertmar et al., 1969; Heim, 1935; Iwai, 1956; Miller, 1969; Nelson, 1967). Many anatomical

studies suggest that the EBO plays a role in the gustation and concentration of food particles that are collected by the gill rakers; it has been suggested that food is trapped by mucus produced by the EBO, concentrated into a bolus, then expelled into the esophagus for consumption (Bauchot et al., 1993; Bertmar et al., 1969; Cohen & Hernandez, 2018; Hansen et al., 2014; Miller, 1964; Pasleau et al., 2010). This hypothesis is supported by numerous observations of food items compacted into mucus-bound boli within the organ and, in some species, the presence of taste buds in the epithelial lining (Cohen & Hernandez, 2018; D'Aubenton, 1955; Hansen et al., 2014; Miller, 1964).

Epibranchial organs (EBOs) have been described in six teleostean orders, with the majority of both morphological and taxonomic diversity of fishes with EBOs occurring within otomorphan fishes (Figure 2a) (Bertmar et al., 1969; Nelson, 1967). Otomorpha is a clade that consists of more than 11,000 marine and freshwater species, including many economically important species, like anchovies and herring (Arratia, 2018; Nelson et al., 2016). It also includes the superorder Ostariophysi, which accounts for over 70% of freshwater fish diversity (Nelson et al., 2016). Not all otomorphan species possess EBOs, though they have been described in four of seven otomorphan orders: Clupeiformes, Gonorynchiformes, Cypriniformes, and Characiformes (Figure 2b) (Bertmar et al., 1969; Cohen et al., 2022; Hansen et al., 2014; Nelson, 1967; Pasleau et al., 2010). Even within these four orders, the presence of an EBO is not ubiquitous, and it is unclear how many times the EBO has evolved. No EBO has been recorded in the early-diverging clupeiform lineages *Denticeps* (Forey, 1975) and Spratelloididae, though they have been described in many distantly related clupeiform lineages. In fact, Clupeiformes is the order with the greatest number of species that possess an EBO (Bertmar et al., 1969). While most gonorynchiforms possess an EBO, the patchy distribution seen in Clupeiformes is reflected in Cypriniformes and Characiformes, where similarly most members do not possess an EBO. This pattern has led researchers to question whether EBOs are homologous structures across Otomorpha or if they have multiple independent origins within the clade (Bertmar et al., 1969; Cohen et al., 2022; Nelson, 1967; Pasleau et al., 2010).

There are conflicting hypotheses regarding the evolutionary origin, function, and morphological diversification of the EBO (Bertmar et al., 1969; Cohen et al., 2022; Nelson et al., 1967; Takahasi, 1957). One hypothesis suggests that EBOs are homologous across Otomorpha, having a single origin in late holosteans and being subsequently lost or reduced in numerous lineages (Bertmar, 1969). Alternatively, EBOs have been hypothesized to be

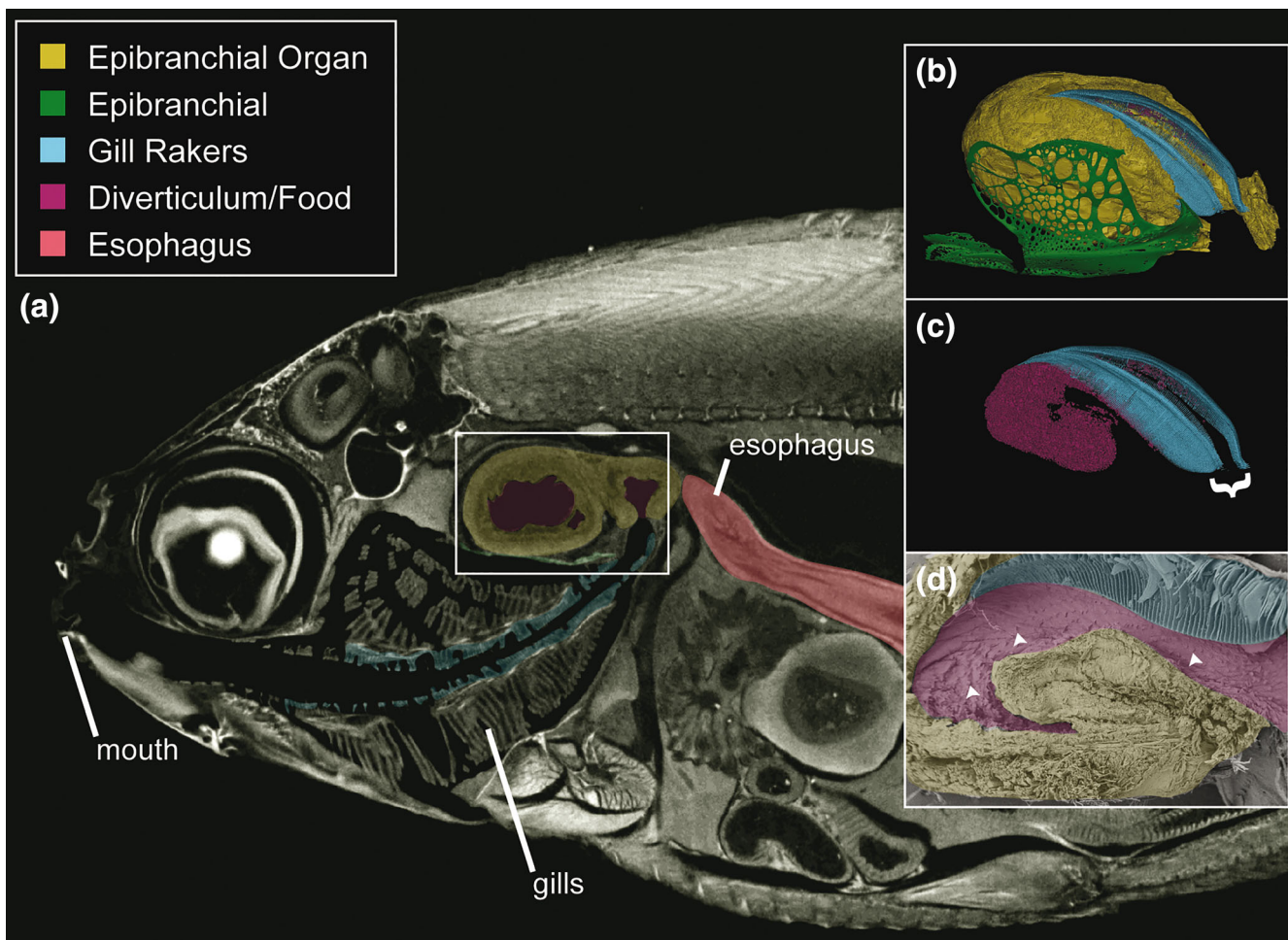


**FIGURE 1** The right epibranchial organ of *Dorosoma cepedianum* (57.8 mm TL). (a) Sagittal section of a contrast-stained μCT. (b) Lateral view of an EBO, depicting skeletal support from the modified fourth epibranchial (green) and associated gill rakers from the medial fourth and single fifth epibranchial (blue) penetrating the muscular wall of the organ (yellow). (c) Lateral view of the EBO with epibranchial support and muscular wall removed. Food contents of the EBO are contoured to the distinctive fish-hook shape of the diverticulum (magenta). White bracket emphasizes the space between the fourth and fifth epibranchials (to which the rakers are attached) that is covered by the cartilaginous capsule. (D) SEM of a bisected EBO showing examples of papillae (arrowheads) studded along the epithelium of the diverticulum.

convergent structures, with multiple independent origins within each of the four otomorphan orders in which they've been described (Nelson, 1967). Recent studies have emphasized the necessity of revisiting classic hypotheses regarding the origin of trophic adaptation (Borstein et al., 2024); this is especially true for EBOs given advances in taxonomic sampling and phylogenetic methods that have changed our understanding of otomorphan evolution over the last 50 years.

For decades, the function and anatomy of otomorphan EBOs have been of interest to morphologists, and the interspecific variation of EBO anatomy has been preliminarily described under a broad array of names (e.g., pharyngeal pocket, pharyngeal pouch, gill-helix, pharyngeal organ, suprabranchial organ) (Bensam, 1964; Bertmar et al., 1969; Boulenger, 1901; Cohen &

Hernandez, 2018; Cohen et al., 2020; Cohen et al., 2022; Hansen et al., 2014; Nelson, 1967; Paselau & Diogo, 2010; Takahasi, 1967). Found in many planktivorous and detritivorous species, the morphological diversity of otomorphan EBOs is vast. EBO anatomy ranges from small pockets (*Anchoa*) to muscularly robust, coiled pouches lined with filamentous papillae (*Chanos*) (Bertmar, 1969; Cohen et al., 2022; Kapoor, 1954). Yet even with such disparate morphologies, they share several anatomical characteristics. The basic structure of EBOs consists of bilaterally paired diverticula (the blind-ended internal sacs within the EBO in which food particles accumulate) lined with an epithelium rich in mucus-producing cells and surrounded by layers of skeletal muscle that are innervated by arborized branches of the vagus nerve (Bertmar et al., 1969; Hansen

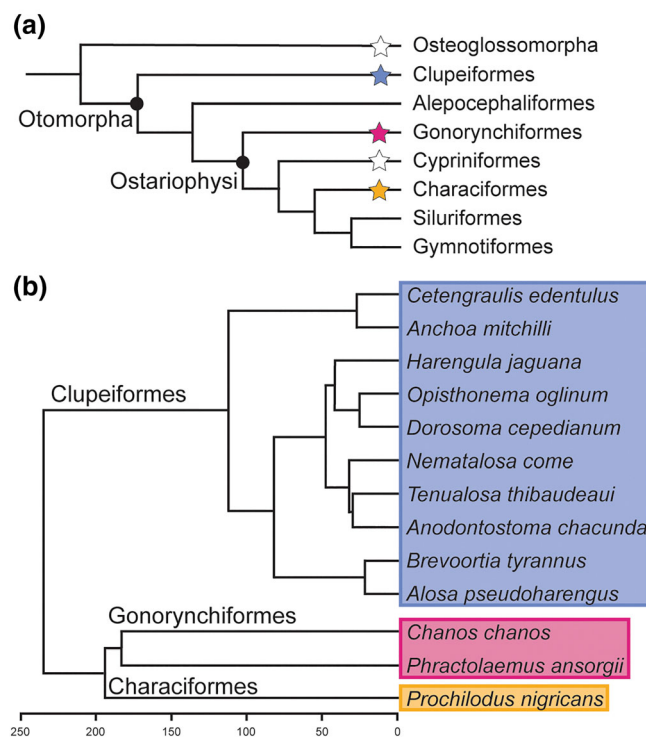


**FIGURE 2** (a) Five incidences of epibranchial organ evolution, demarcated by stars. Note that stars do not indicate an ancestral state, only that epibranchial organs have evolved at least once within this group. Colored stars indicate the three orders sampled from in this study (blue, Clupeiformes; magenta, Gonorynchiformes; orange, Characiformes). Not depicted is the evolution of EBOs in Salmoniformes (Bertmar & Strömberg, 1969). Phylogenetic relationship of orders within Otomorpha is based on Betancur-R et al. (2017) and Straube et al. (2018). (b) Truncated phylogeny based on Egan et al. (2024) of our taxonomic sample, chosen for their presence of EBOs as described in the literature or seen during dissection.

et al., 2014). In most otomorphans, the diverticula are penetrated by the rakers of the medial fourth and the single fifth epibranchial series. Each organ is supported by the highly modified fourth epibranchial bone from which extends a thin piece of cartilage (cartilaginous capsule sensu Bertmar, 1969) that encapsulates the lateral and dorsal aspects of the organ (Bertmar, 1969; Miller, 1969) (Figure 1). These structures are common to all EBOs, a pattern that invites numerous questions about their functional significance: What role do these components play in the aggregation of food, and how might variation in these structures relate to evolutionary history and feeding ecology?

Bertmar et al. (1969) first categorized variation in EBO morphology into seven discrete types of EBO. This effort spanned great taxonomic breadth and was primarily based on gross descriptions collected from multiple studies, each of which focused on different aspects of

EBO morphology with varying degrees of anatomical resolution. This necessary amalgam of sources emphasized the great complexity of the EBO; however, the lack of standardized illustrations and presentation of anatomical details has made comparison of EBOs across species difficult. Furthermore, in the five decades since the study's publication, our understanding of how otomorphan groups are related has changed and is now better informed at finer taxonomic levels by robust molecular phylogenies (Bloom & Lovejoy, 2012; Egan et al., 2018; Egan et al., 2024; Fink & Fink, 1981; Lavoué et al., 2013). Inconsistency in methodologies coupled with a limited phylogenetic framework has hindered our capacity for interspecific comparison, and no study has yet explored how phenotypic diversity of EBOs varies with phylogenetic relatedness or ecology.

The goals of this study are threefold: (1) We characterize otomorphan EBO anatomy at the gross and histological level, identifying common components of EBO architecture to establish a new system for categorizing morphological diversity. (2) We assess the relationship between EBO anatomy, phylogeny, and diet. (3) We interpret our results in the context of EBO evolution and discuss existing hypotheses for the origin of the EBO as a novel feeding structure. To achieve these goals, we compare the gross anatomy and microstructure of the EBOs of 13 species across three otomorphan orders (Clupeiformes, Gonorynchiformes, Characiformes). Our taxonomic sampling includes *Cetengraulis edentulus*, *Nematalosa come*, and *Tenualosa thibaudaeui*, of which the EBO has never been described before. We also present preliminary data from scanning electron microscopy to characterize and compare the internal surface topography of the diverticula of three species: *Brevoortia tyrannus*, *Dorosoma cepedianum*, and *Chanos chanos*. Using updated phylogenies and dietary data collected from existing literature, we preliminarily assess the following hypotheses: (1) similarity in EBO anatomy is best explained by phylogenetic relatedness and (2) similarity in EBO anatomy is best explained by similarity in diet.

## 2 | MATERIALS AND METHODS

### 2.1 | Gross anatomy, histology, micro-CT, and scanning electron microscopy

Frozen and/or formalin-fixed adult and large juvenile specimens representing 13 species across three otomorphan orders were acquired through commercial trade or borrowed from museum collections (Table 1 and Figure 2). Species were selected based on prior

**TABLE 1** Otomorphan species included in this study (order, family, species), museum collection ID or specimen source (specimen), standard length (SL), and number of specimens examined (*n*).

| Order            | Family           | Species                       | Specimen                      | SL (mm) | <i>n</i> |
|------------------|------------------|-------------------------------|-------------------------------|---------|----------|
| Clupeiformes     | Engraulidae      | <i>Cetengraulis edentulus</i> | FMNH 97774                    | 40–44   | 3        |
| Clupeiformes     | Engraulidae      | <i>Anchoa mitchilli</i>       | VIMS 09159                    | 39–41   | 2        |
| Clupeiformes     | Dorosomatidae    | <i>Harengula jaguana</i>      | TCWC 8701.07, 2098.01         | 62–120  | 2        |
| Clupeiformes     | Dorosomatidae    | <i>Opisthonema oglinum</i>    | TCWC 456.04                   | 146–157 | 3        |
| Clupeiformes     | Dorosomatidae    | <i>Dorosoma cepedianum</i>    | commercial trade              | 97–350  | 7        |
| Clupeiformes     | Dorosomatidae    | <i>Nematalosa come</i>        | JFBM 48151                    | 58–62   | 3        |
| Clupeiformes     | Dorosomatidae    | <i>Tenualosa thibaudeaui</i>  | JFBM 48961                    | 96–108  | 3        |
| Clupeiformes     | Dorosomatidae    | <i>Anodontostoma chacunda</i> | JFBM 49207                    | 107–110 | 3        |
| Clupeiformes     | Alosidae         | <i>Brevoortia tyrannus</i>    | Commercial trade              | 60–254  | 7        |
| Clupeiformes     | Alosidae         | <i>Alosa pseudoharengus</i>   | TCWC 5256.01                  | 124     | 1        |
| Gonorynchiformes | Chanidae         | <i>Chanos chanos</i>          | Commercial trade              | 283–345 | 5        |
| Gonorynchiformes | Kneriidae        | <i>Phractolaemus ansorgii</i> | AMNH 240179, commercial trade | 33–127  | 4        |
| Characiformes    | Prochilodontidae | <i>Prochilodus nigricans</i>  | ROM 86141                     | 248–275 | 3        |

Abbreviations: AMNH, American Museum of Natural History; FMNH, Field Museum; JFBM, Bell Museum of Natural History; ROM, Royal Ontario Museum; TCWC, Texas A&M University Biodiversity Research and Teaching Collections; VIMS, Virginia Institute of Marine Sciences.

documentation of the presence of an epibranchial organ in the literature or because the organ was observed during exploratory dissections conducted without a microscope. Clupeiform species were selected to cover distantly related lineages that may potentially represent independent origins of the epibranchial organ or at least unique morphologies, as described by previous studies (Bertmar et al., 1969). Gonorynchiform and characiform species were included to allow for comparison across otomorphan orders. Epibranchial organs and attached branchial arches were dissected out of the pharynx for anatomical examination. Following dissection, photographs were taken of the first gill arch and the posterior gill arches (modified fourth and fifth arches with EBO attached) and then traced for schematic illustrations.

For histological examination, formalin-fixed EBOs were infiltrated with JB-4 following an embedding media protocol from Electron Microscopy Science, sectioned at 2–3 µm, and stained with Lee's Methylene Blue-Basic Fuchsin stain. When size permitted, EBOs were embedded whole. Otherwise, they were cut in half through the midline or embedded in sections with samples taken from the ventral wall of the entrance, the anterior and ventral wall of the approximate middle of the diverticulum, the anterior wall of the medioventral bend, and the ventral wall of the blind end.

Localized measurements of muscularity and adiposity were taken from two-dimensional histological sections of the middle of the diverticulum. This position was chosen as a means of standardizing the sampling across morphologically diverse EBOs, which can vary in absolute

thickness as well as tissue composition along their length. All images were measured in Fiji (version 1.54 m, Schindelin et al., 2012). The thickness of the EBO wall (at our standardized point) was measured as the straight-line distance from the outer edge of the basement membrane to the outer edge of the muscular layer. The thickness of the muscular layer was measured as the straight-line distance between the most superficial bundles of muscle and the deepest bundles. The thickness of the adipose layer (when present) was measured as the straight-line distance from the basement membrane to the inner edge of the muscular layer. A proportion was calculated to approximate how much of the wall was composed of muscle ( $\frac{\text{muscle thickness}}{\text{total thickness}}$ ) and adipose tissue ( $\frac{\text{adipose thickness}}{\text{total thickness}}$ ) at the standardized point. By using a standardized point and using ratios rather than absolute measurements of thickness, we hoped to minimize the effect of any irregularity in the section. It is important to note that this is not a measurement of the total amount of muscle present in the organ, as this would require 3D volumetric data, which is difficult to obtain for some of the smallest organs in our sample (<2 mm).

MicroCT scans were used to visualize the three-dimensional structure of both skeletal and soft-tissue anatomy of the epibranchial organ in *Dorosoma cepedianum*. One whole fish and one dissected EBO (right organ) were fixed in formalin and subsequently stained with iodine (1% w/v iodine, 2% w/v potassium iodide) for 48 h. The specimens were scanned on the Bruker 1173 SkyScan at the Karel F. Liem Bio-Imaging Center at the University of Washington Friday Harbor

Laboratories. The whole fish was scanned at 60 kV and 133 µA; voxel size was 15 µm. The EBO was scanned at 55 kV and 143 µA; voxel size was 15.98 µm. CT scans were segmented in Mimics (version 20.0, Materialize Inc., Leuven, Belgium). Image stacks were uploaded to and made publicly available on the scientific data repository MorphoSource (<https://www.morphosource.org/>). They may be found under the following media numbers: 000720026 (whole fish) and 000720245 (epibranchial organ).

Following anatomical examination, EBOs were scored for the presence and absence of eight anatomical traits (Table 2). These traits were chosen to capture diversity at the gross and histological level. We note that some of these traits were categorized as binary (presence of a coiled diverticulum, presence of muscular islands, muscular investment of the papillae, presence of adipose tissue between the muscular and epithelial layers, presence of rakers from the fourth and fifth gill arches extending into the diverticulum), although variation of the trait exists within our sample. For example, scoring for the presence of a coiled diverticulum (a diverticulum that curves or spirals along the medial face of the EBO) does not capture variation in the length of the coil. Continuous traits (shape, muscularity of the sampled wall, length of raker extension into the diverticulum) were divided into at least two bins that captured both extremes of the variation present within the sample. Muscularity of the sampled EBO wall was binned into three categories (>95% muscle, between <95% and >70% muscle, <70% muscle).

The topography of the internal surface of the EBO was examined with scanning electron microscopy in three species (*D. cepedianum*, *B. tyrannus*, and *C. chanos*), as these were the species that could be readily acquired frozen. EBOs were dissected out from whole, thawed fish and cut into roughly 1 mm × 1 mm × 1 mm sized tissue samples. Samples were taken from the ventral wall of the entrance of the EBO, the middle of the diverticulum, and the medial wall of the terminus (blind end of the diverticulum). Tissues were fixed in 2.5% glutaraldehyde + 1% paraformaldehyde in 0.12 M sodium cacodylate buffer (pH 7.2–7.4) with postfixation of 1 h in 1% osmium tetroxide. After rinsing in water, samples were dehydrated in a graded series of ethanol (15%–100%), critical-point dried with CO<sub>2</sub> in a Tousimis 931 Critical Point Dryer (Rockville, MD, USA), and coated with either iridium or platinum-palladium in a Cressington 208HR Sputter Coater (Watford, UK). Samples were then imaged with an FEI Teneo LoVac SEM (ThermoFisher Scientific, Washington, DC, USA).

## 2.2 | Dietary analysis and statistical methods

To compare diets among species, diet data were collected from quantitative studies that reported the proportions of different prey types in diets (Table 3) (Buchheister & Latour, 2015; Carr & Adams, 1973; Egan et al., 2017; Ewers & Boesel, 1935; Gay et al., 2002; Hiatt, 1947; Jude, 1973; Kohler & Ney, 1980; Kutkuhn, 1958; Lewis & Peters, 1994; Livingston, 1982; Modde & Ross, 1983; Odum & Anuta, 2001; Odum & Heald, 1972; Pouilly et al., 2004; Soe et al., 2021; Stone & Daborn, 1987; Vega-Cendejas et al., 1994; Vega-Cendejas et al., 1997). As no quantitative assessment of *Tenualosa thibaudeau*'s diet could be found, this species was excluded from dietary analysis. Diet data were expressed as % composition of prey types in the diet, regardless of the unit of measure (e.g., % volume, % number, % dry weight) used to quantify diets in the original studies. All studies reported diets as % weight or % volume apart from two. Gay et al. (2002) reported the diets of *Cetengraulis edentulus* as % number, and Egan et al. (2017) reported the diets of *Nematalosa come* as % frequency. Both of these metrics tend to overestimate the importance of small prey items and underestimate the importance of large prey items in diets. However, both of these species exclusively ate small prey items of similar sizes. Thus, we believe that interspecific diet comparisons based on data from Gay et al. (2002) and Egan et al. (2017) % frequency data were transformed so that they totaled 100%, facilitating interspecific diet comparisons. Diet data were collected from adults when possible but were also collected from large juveniles if adult diet data were unavailable.

To perform statistical analyses and interspecific dietary comparisons, prey types were assigned to 1 of 11 prey categories containing functionally and morphologically similar prey (Table 3). Descriptions of diet categories are reported in Table 4. Of the prey categories, 7 comprised at least 1% of the diet of one species and were used to calculate Bray–Curtis dissimilarity between each species, then to group species using hierarchical agglomerative clustering. The remaining four prey categories were all consumed but never comprised >1% of a species' diet; these were grouped into one miscellaneous category called "other." Bray–Curtis dissimilarity was calculated between each species (*vegdist*, method = "bray"), then species were grouped based on diet similarity using hierarchical agglomerative clustering with complete linkage (*hclust*, method = "complete") in the vegan R package (Bray & Curtis, 1957; Legendre & Legendre, 2012; Oksanen et al., 2013). Many previous studies have

TABLE 2 Presence/absence of anatomical traits listed by species.

| Species                       | Shape   |       |          | Relative muscularity of sampled wall |                  |                      |             | Adipose tissue between muscle and epithelium | Rakers from fourth and fifth arch | Rakers extend <1/2 the length of the diverticulum |
|-------------------------------|---------|-------|----------|--------------------------------------|------------------|----------------------|-------------|--|-----------------------------------|---|
|                               | Coiling | Round | Elongate | Muscular investment                  | >95% of papillae | <95% and >70% muscle | <70% muscle |  |                                   |   |
|                               |         |       |          | muscular islands                     | muscle           | muscle               | muscle      |  |                                   |   |
| <i>Cetengraulis edentulus</i> | 0       | 1     | 0        | 0                                    | 1                | 1                    | 0           | 0  | 0                                 | 1   |
| <i>Anchoa mitchilli</i>       | 0       | 0     | 1        | 0                                    | 1                | 1                    | 0           | 0  | 0                                 | 1   |
| <i>Opisthonema oglinum</i>    | 0       | 1     | 0        | 0                                    | 0                | 1                    | 0           | 0  | 1                                 | 0   |
| <i>Harengula jaguana</i>      | 0       | 0     | 1        | 0                                    | 1                | 1                    | 0           | 0  | 1                                 | 0   |
| <i>Dorosoma cepedianum</i>    | 1       | 1     | 0        | 1                                    | 0                | 0                    | 1           | 0  | 1                                 | 1   |
| <i>Nematalosa come</i>        | 1       | 1     | 0        | 0                                    | 0                | 0                    | 1           | 0  | 1                                 | 0   |
| <i>Tenuilosa thibaudaeui</i>  | 1       | 1     | 0        | 1                                    | 0                | 0                    | 1           | 0  | 1                                 | 0   |
| <i>Anodontostoma chaundra</i> | 1       | 1     | 0        | 0                                    | 0                | 0                    | 0           | 1  | 1                                 | 0   |
| <i>Breviorita tyranus</i>     | 0       | 0     | 1        | 0                                    | 0                | 0                    | 0           | 1  | 1                                 | 0   |
| <i>Alosa pseudoharengus</i>   | 0       | 0     | 1        | 0                                    | 0                | 1                    | 0           | 0  | 1                                 | 1   |
| <i>Chanos chanos</i>          | 1       | 1     | 0        | 0                                    | 0                | 0                    | 0           | 1  | 1                                 | 0   |
| <i>Phractolaemus ansorgii</i> | 0       | 1     | 0        | 0                                    | 0                | 1                    | 0           | 1  | 1                                 | 0   |
| <i>Prochilodus nigricans</i>  | 0       | 0     | 1        | 1                                    | 0                | 0                    | 0           | 1  | 0                                 | 1   |

**TABLE 3** Diet composition of 12 species expressed by relative occurrence of 11 prey categories: Algae (Alga), Annelids (Anne), Crustaceans (Crus), Detritus (Detr), Eggs (Egg), Fish (Fish), Mollusks (Moll), Phytoplankton (Phyt), Plants (Plan), Terrestrial Invertebrates (Terr), Zooplankton (zoop).

| Species                       | Alga  | Anne  | Crus  | Detr  | Egg   | Fish  | Moll  | Phyt  | Plan  | Terr  | Zoop  | Citations  |
|-------------------------------|-------|-------|-------|-------|-------|-------|-------|-------|-------|-------|-------|--|
| <i>Cetengraulis edentulus</i> | 0.039 | 0     | 0     | 0     | 0.001 | 0     | 0     | 0.953 | 0     | 0     | 0.004 | Gay et al., 2002   |
| <i>Anchoa mitchilli</i>       | 0     | 0     | 0.254 | 0     | 0.019 | 0     | 0     | 0     | 0.043 | 0.019 | 0.665 | Odum & Heald, 1972; Carr & Adams, 1973; Livingston, 1982             |
| <i>Opisthonema oglinum</i>    | 0     | 0     | 0.356 | 0.314 | 0     | 0.057 | 0.016 | 0.037 | 0.151 | 0     | 0.068 | Vega-Cendejas et al., 1997   |
| <i>Harengula jaguana</i>      | 0.01  | 0.083 | 0.424 | 0.006 | 0     | 0.246 | 0.003 | 0.13  | 0     | 0     | 0.097 | Modde & Ross, 1983; Vega-Cendejas et al., 1994                       |
| <i>Dorosoma cepedianum</i>    | 0     | 0     | 0.006 | 0.563 | 0     | 0     | 0.061 | 0.043 | 0     | 0     | 0.327 | Ewers & Boesel, 1935; Kutkuhn, 1958; Jude, 1973                      |
| <i>Nematalosa come</i>        | 0.167 | 0     | 0.023 | 0.32  | 0.097 | 0     | 0     | 0.25  | 0.037 | 0     | 0.107 | Egan et al., 2017  |
| <i>Anodontostoma chacunda</i> | 0     | 0.026 | 0     | 0     | 0     | 0     | 0     | 0.419 | 0     | 0     | 0.556 | Soe et al., 2021   |
| <i>Brevoortia tyrannus</i>    | 0     | 0     | 0     | 0.748 | 0     | 0     | 0     | 0.11  | 0.011 | 0     | 0.128 | Lewis & Peters, 1994   |
| <i>Alosa pseudoharengus</i>   | 0     | 0.009 | 0.477 | 0     | 0     | 0     | 0     | 0     | 0     | 0.103 | 0.412 | Kohler & Ney, 1980; Stone & Daborn, 1987; Buchheister & Latour, 2015 |
| <i>Chanos chanos</i>          | 0.237 | 0     | 0     | 0.113 | 0     | 0     | 0     | 0.443 | 0.144 | 0     | 0.031 | Hiatt, 1947  |
| <i>Phractolaemus ansorgii</i> | 0.096 | 0.043 | 0.023 | 0.489 | 0     | 0.02  | 0     | 0.202 | 0.092 | 0     | 0.035 | Odum & Anuta, 2001   |
| <i>Prochilodus nigricans</i>  | 0.581 | 0     | 0     | 0.323 | 0     | 0     | 0     | 0     | 0.032 | 0.065 | 0     | Pouilly et al., 2004   |

arbitrarily chosen a similarity index value of 40% as the basis for dividing species into trophic groups (Horinouchi et al., 2012; Horinouchi & Sano, 2000; Inoue et al., 2005; Nakamura et al., 2003; Nanjo et al., 2008). In congruence with these studies, a critical dissimilarity cutoff of 60% was adopted, as dissimilarity = 1 – similarity.

A co-phylogenetic approach was used to assess patterns of evolutionary relatedness and anatomical diversity. As no published phylogeny included all species examined in this study, the most recent and comprehensive molecular clupeiform phylogeny available (Egan et al., 2024) was used as the phylogenetic framework for our analysis. This phylogeny included a gonorynchiform (*Chanos chanos*) and characiform (*Astyanax mexicanus*) outgroup, the latter of which was used as a substitute for *Prochilodus nigricans* since the divergence time estimate for species within the order would be the same.

*Phractolaemus ansorgii* was incorporated into the tree with the phytools R package function *bind.tip* (Revell, 2024) using the divergence time estimate from Near et al. (2014). The phylogeny was then pruned to contain only sampled clupeiform taxa. Since genera sampled in this study were identified as monophyletic (with the exception of *Anchoa*) and we did not compare any taxa within the same genus, when species were not present, they were substituted with a congener. Species were clustered according to their anatomical similarity (presence/absence of discrete EBO characters; Table 2) using a UPGMA analysis as implemented by the *hclust* and *pvcclus* functions (vegan and pvcclus R packages; Oksanen et al., 2013; Suzuki & Shimodaira, 2006). Anatomical similarity was reported as a percentage determined by the AU (approximately unbiased) *p*-values for each node in the cluster dendrogram following the

**TABLE 4** Prey types in each prey category (not taxonomic) used for agglomerative cluster analyses of diets.

| Prey category                    | Prey category composition  |
|----------------------------------|--|
| Algae (Alga)                     | Acrochaetium, benthic periphyton, benthic biofilm, Chlorophyta, Chrysophyceae, Cladophora, Cyanophyceae, cyanobacteria, filamentous algae, Vaucheria |
| Annelids (Anne)                  | Annelida, Polychaeta   |
| Crustaceans (Crus)               | Amphipoda, Apseudidae, Brachyura, crab, Crustacea, Cumacea, Decapoda, Gammaridea, Isopoda, Mysidae, shrimp   |
| Detritus (Detr)                  | Detritus, mud  |
| Eggs (Egg)                       | Egg, fish egg  |
| Fish (Fish)                      | Fish, teleost  |
| Mollusks (Moll)                  | Benthic Bivalva, Bivalva, Gastropoda, Mollusca   |
| Phytoplankton (Phyt)             | Centric diatom, diatom, Dinoflagellata, pennate diatom, phytoplankton  |
| Plants (Plan)                    | Plant, macrophyte fragment   |
| Terrestrial Invertebrates (Terr) | Insecta, terrestrial Insecta   |
| Zooplankton (Zoop)               | Copepoda, Calanoida, Cladocera, Harpacticoida, Ostracoda, zooplankton, zooplankton veliger   |

*Note:* Prey types are shown as they appeared in the original articles from which we collected diet data, except for where we updated taxonomy. In some cases, prey types are redundant (e.g., “Brachyura” and “crab”) or nested due to inter-study differences in taxonomic resolution (e.g., “Annelida” and “Polychaeta”), highlighting a key motivation for condensing prey types into more general prey categories prior to statistical analyses.

methods outlined in Cohen et al. (2023). The *cophylo* function in the phytools R package (Revell, 2024) was then used to render a tanglegram that compares the configuration of the phylogeny and the dendrogram of EBO anatomical similarity. All statistical analyses were conducted in R (version 4.2.1, R Core Team, 2022).

### 3 | RESULTS

All epibranchial organs (EBOs) consist of muscular, bilaterally paired diverticula (blind-ended internal sacs in which food particles accumulate). The anterior end of the organs is angled toward the midline of the pharynx and exhibits some degree of antero-ventral flexure along their proximodistal axis. The opening of each organ is located immediately anterior to the esophageal opening and dorsal to the posterior branchial arches (Figure 1a). The fourth and fifth epibranchial series and associated gill rakers extend into the diverticula of the organ in all species but *P. nigricans*. In many clupeiforms, a cartilaginous capsule extends from the dorsal aspect of the supporting fourth epibranchial over the lateral face of the organ, where it is loosely attached to the base of the rakers that enter the EBO. This cartilaginous capsule extends dorsally to varying degrees to partially encapsulate the organ. Though varying widely in their gross anatomy, EBOs share the same basic histological composition, which includes peripheral layers of skeletal muscle, often interspersed with adipose tissue, mucus-producing

epithelial cells lining the inner surface of the diverticulum, and internal papillae covered by said epithelium.

#### 3.1 | Axes of morphological variation

We identify five axes along which EBOs varied in gross anatomy and histological architecture that best explain their breadth of morphological diversity.

##### 3.1.1 | Shape

Epibranchial organs range in shape from spherical and rotund (*C. edentulus*) to elongate and digitiform (*P. ansorgii*) (Figures 3, 4a, and 5d). Rounder EBOs sit atop the branchial arches such that their long axis (proximal-distal) is oriented horizontally; their diverticula, when of considerable length, extend toward the midline of the pharynx with some degree of coiling (curving or spiraling of the diverticulum along the medial face of the organ). Some round, spherical EBOs, such as those of *C. edentulus* and *O. oglinum*, possess a diverticulum that is sac-like; while narrow at the entrance, the diverticulum opens into a wide, spacious chamber-like pocket that roughly reflects the EBO’s external shape and terminates in a ventrally directed blind end (Figure 4a,b). Other EBOs, such as those of *N. come*, *A. chacunda*, *C. chanos*, and *D. cepedianum*, are round to oval-shaped but possess a diverticulum that

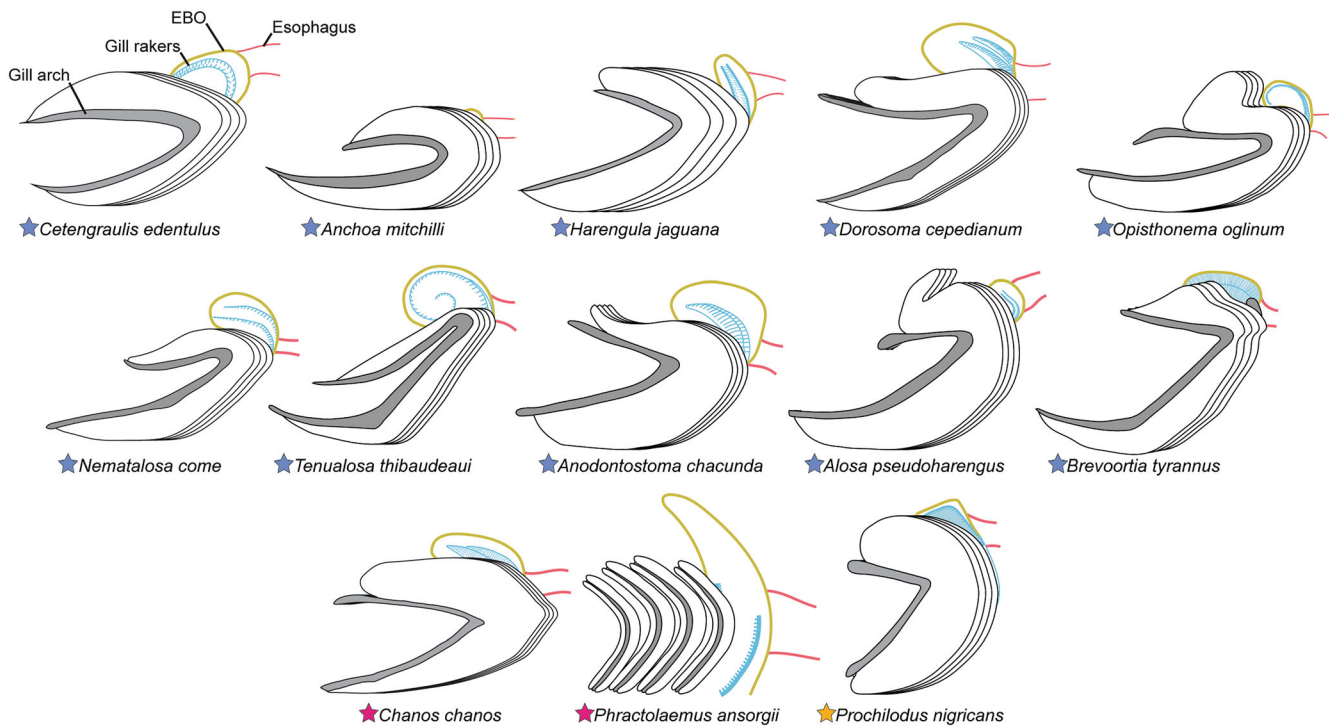


**FIGURE 3** Schematics of gill arches and EBOs based on gross dissection (with cartilaginous capsules removed). Note that these illustrations are from a lateral perspective and do not fully capture the mediolateral dimension, as many EBOs curve medially toward the midline of the pharynx. The body of the EBO is colored yellow. Gill rakers penetrating into the EBO are colored blue. The esophagus is colored orange. Colored stars beside species names indicate TAXONOMIC order (blue, Clupeiformes; magenta, Gonorynchiformes; orange, Characiformes; see Figure 2).

bends medioventrally in an incomplete, J-shaped whorl, which terminates in a posteriorly directed blind end (Figure 4c–f). In *N. come*, *A. chacunda*, and *C. chanos*, the diverticulum is narrow and tubular. In *D. cepedianum*, the diverticulum is wider and the blind end more spacious, similar to the condition of *C. edentulus* and *O. oglinum*. In *N. come*, *A. chacunda*, *C. chanos*, and *D. cepedianum*, the diverticulum coils medioventrally and is externally visible as a muscular protuberance on the medial face of the organ (Figure 4c,g). The diverticulum of *T. thibaudeau* is the most coiled in our sample (Figure 4g), completing a full rotation that terminates in an anteriorly directed blind end.

The remaining six EBOs are more elongate than rotund and lack the extensive coiling exhibited by species such as *A. chacunda* and *T. thibaudeau*. These elongate EBOs exhibit more variation in their orientation relative to the gill arches, with *A. mitchilli*, *B. tyrannus*, and *P. nigricans* oriented horizontally along their proximodistal axis and *A. pseudoharengus*, *H. jaguana*, and *P. ansorgii* oriented vertically (Figures 3 and 5). The EBOs of *A. mitchilli* and *B. tyrannus* are cylindrical and of mostly uniform width along their length (Figure 5a,e), whereas the EBO of *P. nigricans* is pyramidal and tapered toward the terminus (Figure 5f). The diverticula of

*A. mitchilli* and *P. nigricans* are narrow, whereas the diverticulum of *B. tyrannus* is wide and sac-like. In all three, the EBO is curved ventrally at the distal extreme. The EBOs of *A. pseudoharengus*, *H. jaguana*, and *P. ansorgii* are cylindrical with concave curvature and an anteriorly directed distal end (Figure 5b–d). Of these three, the EBO of *A. pseudoharengus* is proportionally the shortest and widest, with a sac-like diverticulum. The EBO of *H. jaguana* is slightly longer and narrower, and the EBO of *P. ansorgii* is the longest, curving medially over the gill arches (see Figure 3 for note).

### 3.1.2 | Size relative to the branchial basket

The size of the epibranchial organ refers to three dimensions: height, length, and depth, only the former two of which are captured in our two-dimensional illustrations (Figure 3). Round, coiling EBOs are proportionally the largest in terms of width and depth, with both round, sac-like EBOs and elongate EBOs being much smaller, if not in width, then in depth. The most obvious exception to this is *P. ansorgii*, whose EBO is proportionally the tallest of our sample. This height is obscured in situ because the EBO is folded medially over the gill arches.

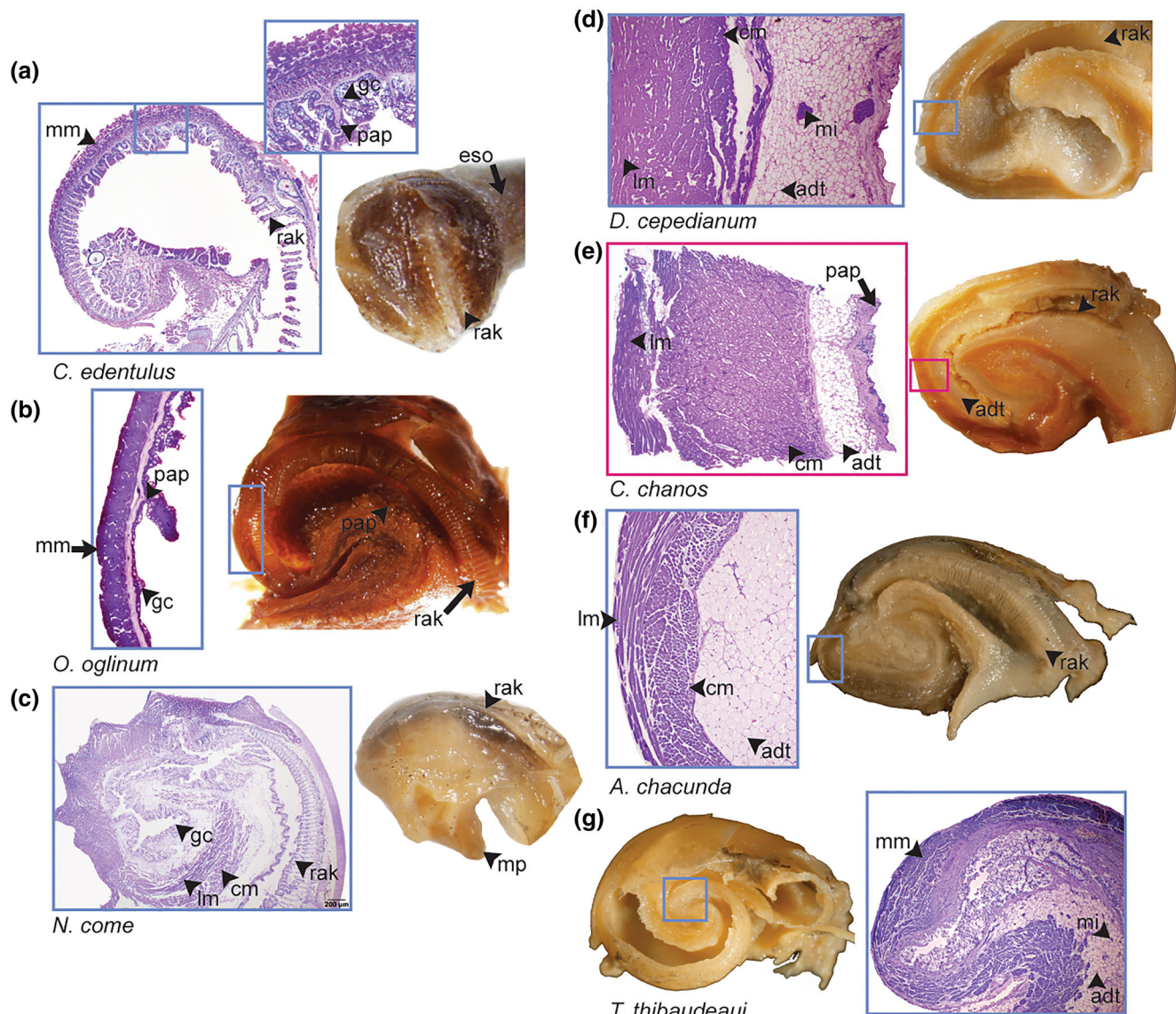


**FIGURE 4** Histological sections and photographs of “round” epibranchial organs dissected out of the pharynx and with ventral gill arch elements and cartilaginous capsule removed. Photographs were taken from a lateral perspective of a single organ, with the exception of *T. thibaudeau*, which was photographed to show the medial face and coiling diverticulum. Note that in (a) and (c), the entire (undissected) organ is photographed to capture its lateral face, whereas in (b) and (d–g), the EBO has been dissected to reveal the shape of the diverticulum. Colored boxes denote the TAXONOMIC order of the species (see Figure 2) and from where in the EBO the histological section was taken. adt, adipose tissue; cm, circumferential muscle; eso, esophagus; gc, goblet cells; lm, longitudinal muscle; mi, muscle island; mm, muscle; mp, muscular protuberance; pap, papillae; rak, rakers.

### 3.1.3 | Gill raker morphology and raker length relative to the length of diverticula

All EBOs are penetrated by the fourth and fifth gill arches with the exception of *P. nigricans*, in which only the fifth arch extends into the EBO. In all species, the dorsal elements of the arch from which the rakers extend are embedded within the walls of the EBO, attaching to a layer of muscle or connective tissue rather than the cartilaginous capsule (cc) directly (Figure 6a–c). In round

EBOs, the rakers from the fourth and fifth arches extend into the EBO in two discrete rows along the dorsolateral aspect of the organ and curve ventrally, following the curvature of the diverticulum (Figures 1b–d and 4). The exception to this is *C. edentulus*, which, like the elongate EBOs of *A. pseudoharengus* and *H. jaguana*, penetrates the organ along the lateral wall (Figures 4a and 5b,c). In clupeiforms, the space between the two rows of rakers (Figure 1b bracket) is either covered by branchial cartilage of the cartilaginous capsule or left as an open

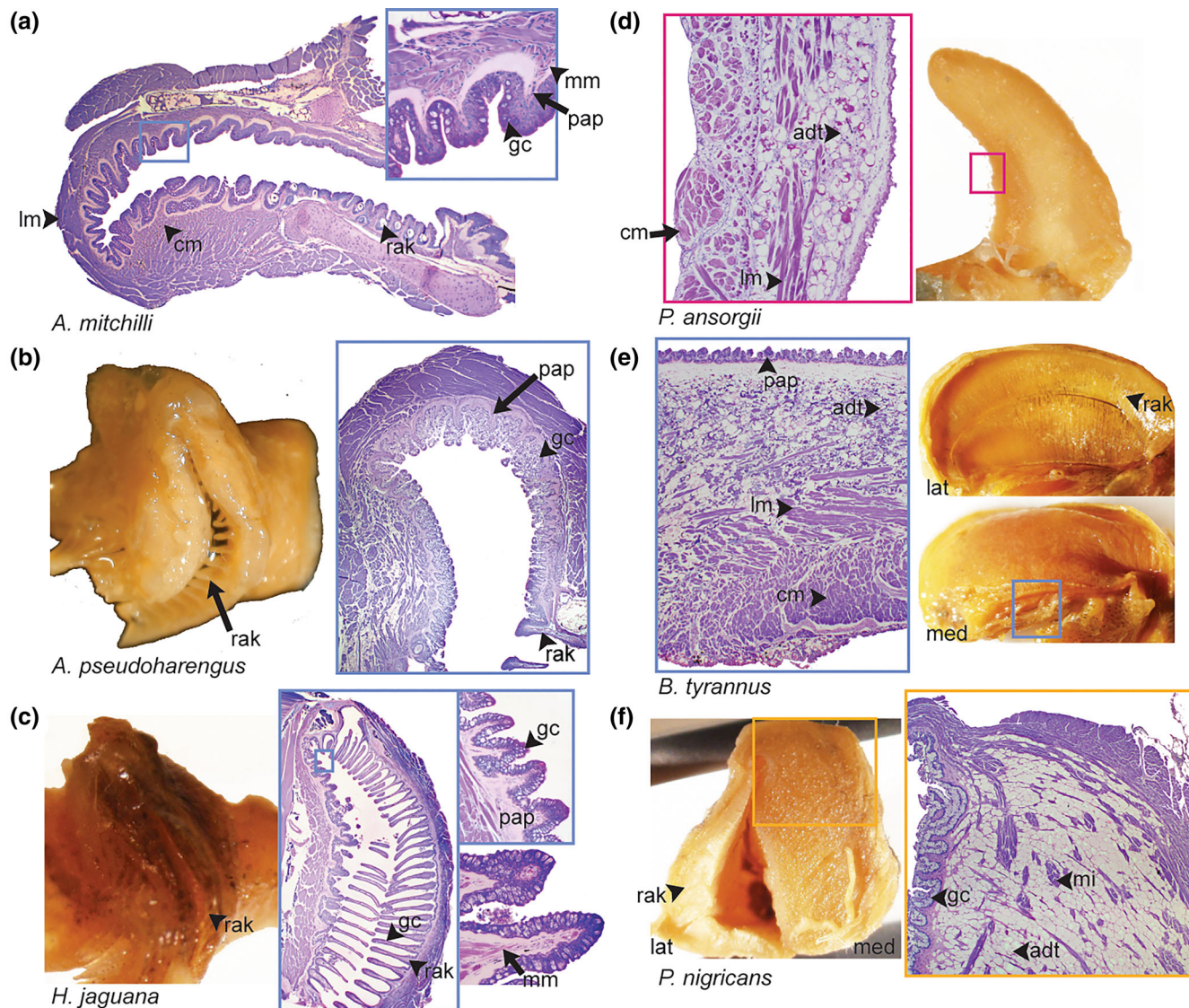


**FIGURE 5** Histological sections and photographs of “elongate” epibranchial organs dissected out of the pharynx and with ventral gill arch elements and cartilaginous capsule removed. Photographs were taken from a lateral perspective of a single organ, with the exception of *A. mitchilli*, which was too small (~2 mm) to provide an informative depiction of the external morphology. (b–d) Photographs taken of an entire undissected organ from the lateral perspective. (e) Photographs of a bisected organ, showing both the lateral wall (lat) and the medial wall (med). (f) Photograph of a cross-section through the center of the organ. Note that the lateral image has been reflected to point anteriorly. Colored boxes denote the TAXONOMIC order of the species (see Figure 2) and from where in the EBO the sample was taken. adt, adipose tissue; cm, circumferential muscle; gc, goblet cells; lat, lateral wall; lm, longitudinal muscle; med, medial wall; mi, muscle island; mm, muscle; pap, papillae; rak, rakers.

gap that is visible externally, as seen in *A. pseudoharengus* and *H. jaguana* (Figure 5b,c). In *C. chanos*, the rakers are completely covered by the muscular wall; the cartilaginous capsule does not extend over them. In *P. ansorgii* and *P. nigricans*, the cartilaginous capsule is absent. In *P. ansorgii*, the rakers and their supporting cartilaginous elements are entirely covered by the walls of the EBO (Figure 6e), while the rakers of *P. nigricans* are distinct in that they constitute the entirety of the lateral wall of the organ (Figure 5f). Regardless of EBO orientation, the rakers point toward the midline of the diverticulum.

Rakers vary in shape, relative density, and in the morphology of their epithelial lining. The epithelium is often studded with goblet cells, though we note that in some specimens the epithelial layers have been damaged or degraded during preservation (*N. come*, *T. thibaudeau*, *P. ansorgii*), making cellular composition difficult to determine. In *A. mitchilli*, the rakers are short and nodular, rarely extending past the surrounding soft tissue (Figure 5a). In *A. chacunda*, *N. come*, and *H. jaguana*, the bony portion of the rakers is narrow and straight, their epithelial lining lending them a slightly spatulate

appearance (Figure 6a,b,d). The rakers of *P. ansorgii* are also narrow and slightly spatulate but distinctly curved; from the base, the raker extends ventrally, curving dorsally where the epithelium begins to thicken to terminate in a tapered point (Figure 6e). The rakers of *B. tyrannus* possess a thin epithelial lining that lacks the presence of goblet cells; the rakers are comparably broader and tri-radiate (Figure 6c). There is also variation in the relative density of rakers, with the rakers of *A. chacunda* and *N. come* having the least space between them (Figure 6a,b). The rakers of *P. nigricans* are highly modified, lacking bony elements and instead supported by muscular bundles and other connective tissue at the base of each raker (Figure 6f).

The length that gill rakers penetrate into the diverticulum also varies, with some rakers terminating approximately  $\frac{1}{3}$  to  $\frac{1}{2}$  of the length of the diverticulum (*C. chanos*, *P. ansorgii*, *A. mitchilli*, *N. come*, *D. cepedianum*, *A. chacunda*) and some extending all the way to the terminus (*C. edentulus*, *O. oglinum*, *T. thibaudeau*, *A. pseudoharengus*, *H. jaguana*, *B. tyrannus*, *P. nigricans*) (Figure 3).

### 3.1.4 | Muscularity

In all examined species, we observed skeletal muscle arranged in layers of circumferential and longitudinal

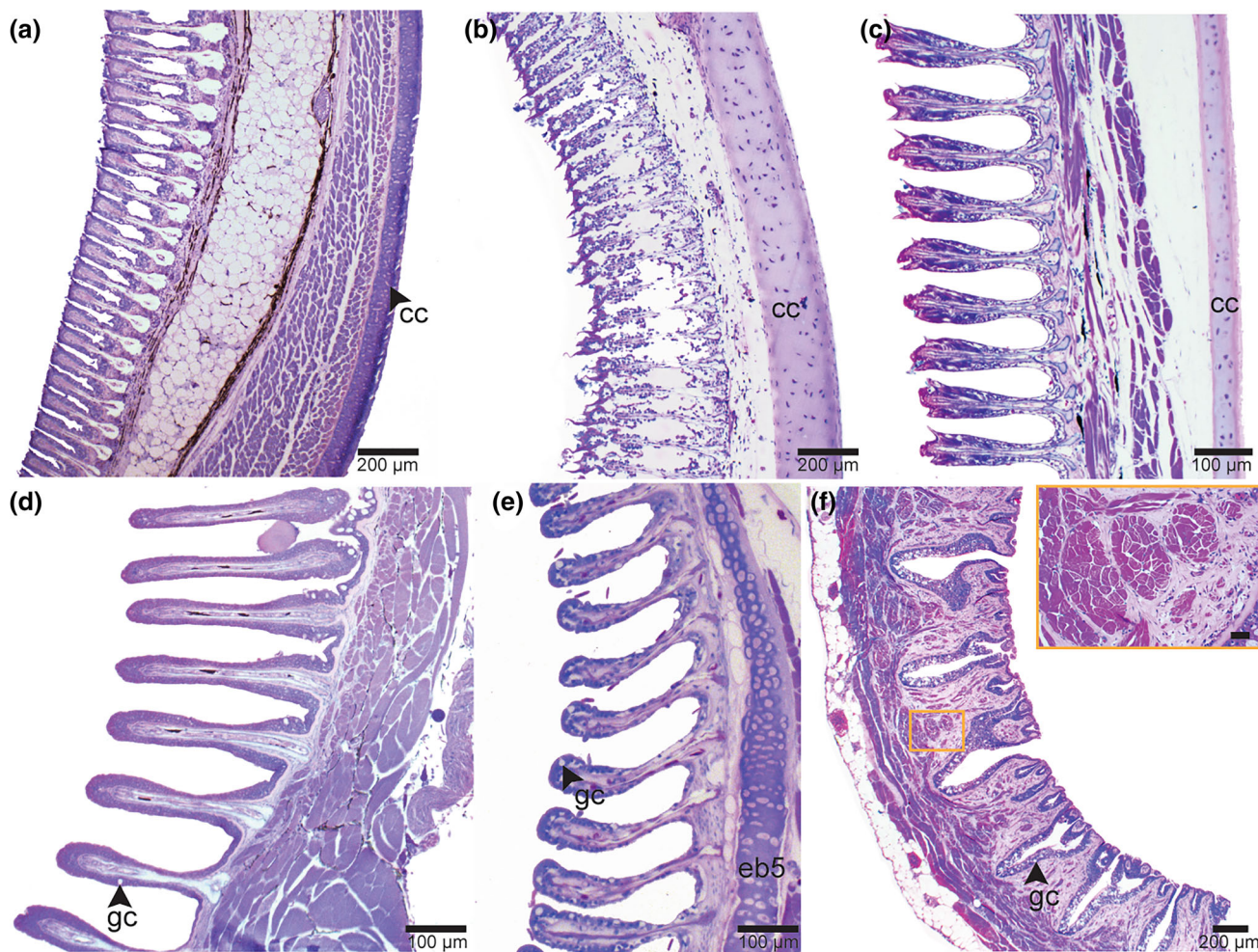


**FIGURE 6** Gill rakers of the medial fourth and fifth epibranchial associated with the epibranchial organs of *Anodontostoma chacunda* (a), *Nematalosa come* (b), *Brevoortia tyrannus* (c), *Harengula jaguana* (d), *Phractolaemus ansorgii* (e), and *Prochilodus nigricans* (f). Gill rakers of the fourth and fifth epibranchial extend into the EBO except in *P. nigricans*, in which only the rakers of the fifth arch are present. The cartilaginous capsule (cc) extends from the fourth epibranchial over each organ and covers the space between the two rows of rakers. A layer of epithelium studded with goblet cells (gc), covers the rakers in most but not all species. Note that due to specimen preservation, this epithelial layer is partially detached and/or degraded in *N. come*. The cartilaginous element of the fifth epibranchial (eb5) can be seen in the posterior wall of *P. ansorgii*'s EBO. The rakers of *P. nigricans* are highly modified with no visible bony elements. At the base of each raker are extensive muscle fibers. Some of these fibers are arranged in stacked bundles (inset, scale bar = 20  $\mu$ m). The loose fibers throughout the connective tissue of the rakers appear to extend medially, toward the terminus of the raker.

fibers. These layers are readily distinguishable in *A. chacunda* and *C. chanos*, with the longitudinal fibers forming the outermost muscular layer and the circumferential fibers forming the inner layer (Figure 4e,f). Not all species, however, have such a discrete organization of muscle fibers; *A. mitchilli*, *A. pseudoharengus*, and *N. come* have regions in which fibers appear to overlap with one another or have fibers arranged at oblique angles to one another. Furthermore, while most EBOs have muscular walls organized such that the layer of circumferential fibers is deep to the layer of longitudinal fibers, in *P. ansorgii*, *B. tyrannus*, and *H. jaguana*, this order is reversed, with the circumferential fibers composing the outermost layer and the longitudinal fibers forming the inner layer (Figure 5c–e).

Relative thickness of the muscular layer varies greatly as well (Table 2); at our measured points, muscular tissue constitutes anywhere between 15% (*P. nigricans*; Figure 5f) of the EBO's wall to nearly 100% (*C. edentulus*; Figure 4a). Round, sac-like EBOs are composed almost entirely of muscular tissue, yet in the sections measured, their walls appear to be thinner than those of the round, coiling EBOs (Figure 4a–g). Round, coiling EBOs have comparably robust walls, with muscular layers that constitute between 50% and 71% of the wall (Figure 4c–g). Elongate EBOs are comparably diverse. At the sampled region, the walls of *A. mitchilli*, *H. jaguana*, and *A. pseudoharengus* are composed mostly of muscle. By contrast, muscle constitutes 15%–78% of the wall in *P. ansorgii*, *B. tyrannus*, and *P. nigricans*.

While in all species, the rakers are embedded in the lateral to dorsolateral wall of the EBO, in both *P. nigricans* and *B. tyrannus*, the lateral wall is composed primarily of rakers (Figure 5e,f). In *B. tyrannus*, this lateral muscular layer is thin (Figure 6c). In *P. nigricans*, these muscular layers are more complex; the outermost layer is composed of circumferential fibers, and deep to this are both longitudinal fibers arranged in muscular bundles and numerous, thin transverse fibers investing the connective tissue of the rakers, some extending all the way to the terminus of the raker (Figure 6f).

In many clupeiform species (*C. edentulus*, *A. mitchilli*, *O. oglinum*, *H. jaguana*, *A. pseudoharengus*), the innermost muscular layer is connected directly to the epithelial layer (Figures 4a,b and 5a–c). In others (*N. come*, *D. cepedianum*, *A. chacunda*, *T. thibaudeau*, *B. tyrannus*), there is a substantial amount of adipose and other connective tissues separating these layers; this is also the case for both gonorynchiform species and the medial wall of *P. nigricans* (Figures 4c,d,f,g and 5d–f). In *D. cepedianum*, *T. thibaudeau*, and the medial wall of *P. nigricans*, bundles of isolated muscle fascicles (muscle

islands) are interspersed throughout the adipose tissue between the muscular and epithelial layers. These muscle islands vary in size within the specimen. In *P. nigricans*, some of these muscle fibers attach to the epithelial layer. Of note, we find muscle fibers connecting directly to individual papillae in several species, including *C. edentulus*, *H. jaguana*, and *A. mitchilli* (Figures 4a and 5a,c).

### 3.1.5 | Adiposity

Adipose tissue is the most abundant connective tissue present in the walls of the EBOs. As with muscular layers, the adipose layer varies in relative thickness across species at the measured point, with the most fatty EBOs represented by the round, coiling EBOs as well as *P. nigricans*. Adipose tissue is found in between muscle and epithelium, between muscular layers, and in between muscle fascicles. In most species, the layer of adipose tissue is thinner than that of the muscle, with the exception of *A. chacunda* and *P. nigricans*, the latter of which is notable in that most of its medial wall is composed of adipose tissue interspersed with muscle islands (Figure 5f). In thin-walled EBOs (*C. edentulus*, *O. oglinum*, *H. jaguana*), little to no adipose tissue is present (Figures 4a,b and 5c).

## 3.2 | Internal topography of the diverticula

In all three examined species, the interior of the diverticulum is covered with papillae that are directed toward the terminus (the blind end of the diverticulum). These papillae vary in length, shape, and density; these characteristics also vary at different positions along the proximal-distal axis of the diverticulum (Figure 7). Papillae in *D. cepedianum* are short, wide, and nodular in appearance (Figure 7a, arrowheads). Proximally (at the opening of the EBO), they can be found grouped together on protruding ridges but appear more isolated in distal (at the blind end of the diverticulum) sections (Figure 7d). Papillae in *B. tyrannus* are thinner and become longer and more filamentous toward the distal end of the diverticulum (Figure 7d–f). Papillae in *C. chanos* are the most morphologically diverse of the species examined in this study. At the proximal end, they appear as circular nodules or lingulate papillae of varying lengths and sizes (Figure 7g). Many of the more circular papillae are oriented upright and flat with their dorsal aspect roughly level with the surrounding folds of tissue (Figure 7g, circle), while others are slightly rounded on top. The lingulate papillae are much longer and folded over on themselves (Figure 7g).

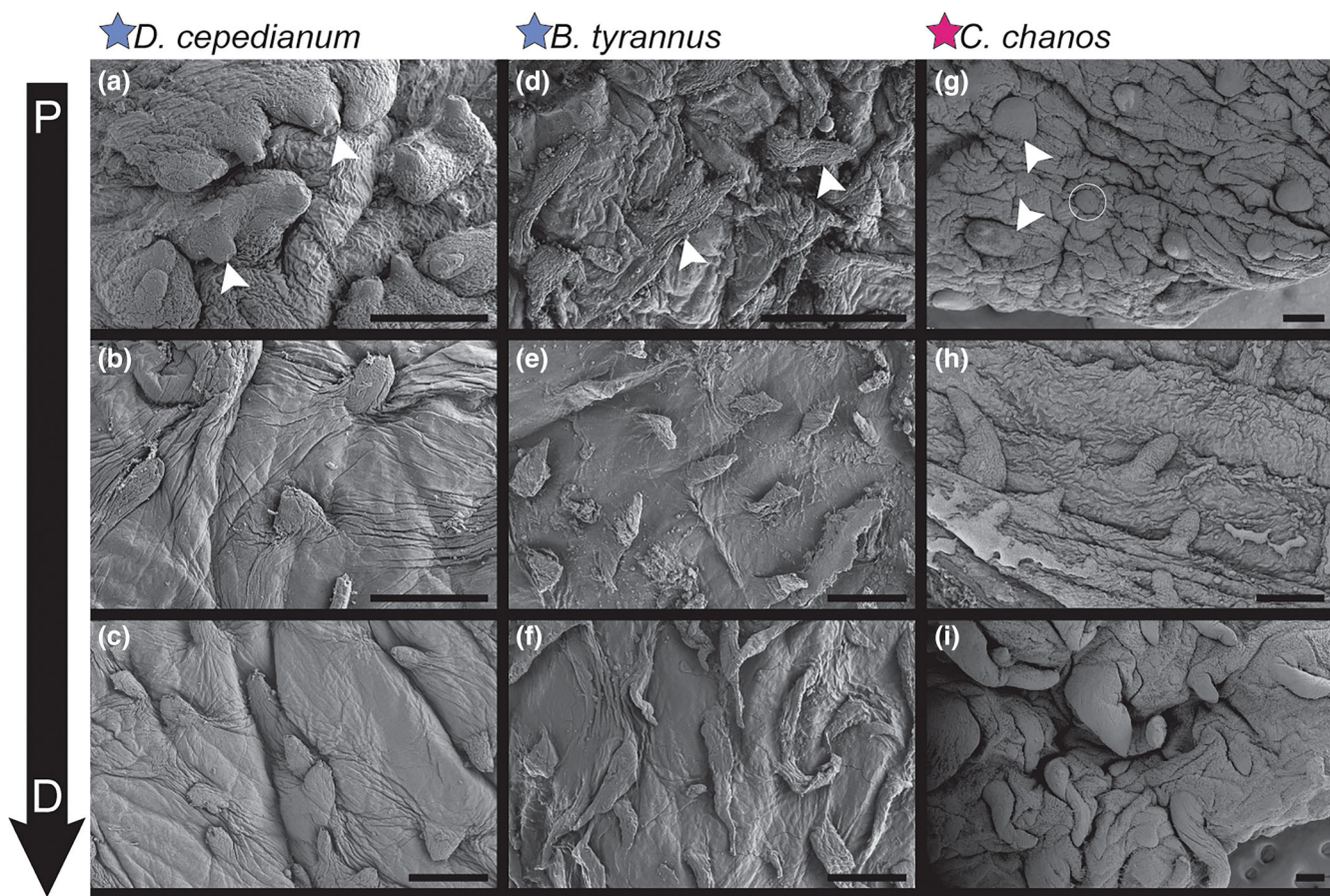


**FIGURE 7** Electron micrographs of the internal surface of the diverticulum in three species. *D. cepedianum* (a–c, scale bar at 100 µm), *B. tyrannus* (d–f, scale bar at 100 µm), and *C. chanos* (g–i, scale bar at 200 µm). For each species, micrographs were taken at different positions along the length of the diverticulum (entrance, approximate middle, and terminus) and are displayed from proximal (P) to distal (D) in each column. Examples of papillae in each of the three species are marked by white arrowheads. Note that in *C. chanos*, some papillae are short, round, and roughly level with the surrounding folds of tissue (circle).

arrowheads). These lingulate papillae are wide at the base and taper to a softly pointed tip, giving them a broadly triangular or tongue-shaped appearance. Further distally, the papillae are longer and thicker, especially at the terminus of the diverticulum, where they are large enough to be visible under a light microscope (Figure 7i).

### 3.3 | Relationship between morphology, diet, and phylogeny

We identified six general prey groupings that can be summarized by species feeding primarily on (1) phytoplankton, (2) crustaceans and zooplankton, (3) crustaceans and a second prey type, (4) detritus, (5) algae (in the taxa examined the algae consumed almost exclusively consisted of small algae/algal fragments (Table 4)), and (6) a combination of algae, detritus, and phytoplankton (Figure 8).

We found a mismatch between phylogenetic relatedness and anatomical similarity, as indicated by the lack

of correspondence (crossing) of connecting lines on the tanglegram (Figure 9). Species feeding on crustaceans clustered together, all of which exhibited little adipose tissue and anterior walls composed primarily (>95%) of muscle (Table 2). This is also the condition found in the EBO of *C. edentulus*, a phytoplanktivore. The other clusters are more dietarily diverse. Round, coiling EBOs clustered together with strong anatomical similarity (>90%). Within this cluster, pairs like *C. chanos* + *A. chacunda* and *D. cepedianum* + *N. come* all had diets characterized by large quantities of detritus and either algae, phytoplankton, or both (Figure 8).

## 4 | DISCUSSION

In this study, we characterized the anatomical diversity and histological structure of the epibranchial organ (EBO) in 13 otomorphan species. This included *Cetengraulis edentulus*, *Tenualosa thibaudeau*, and *Nematalosa come*,

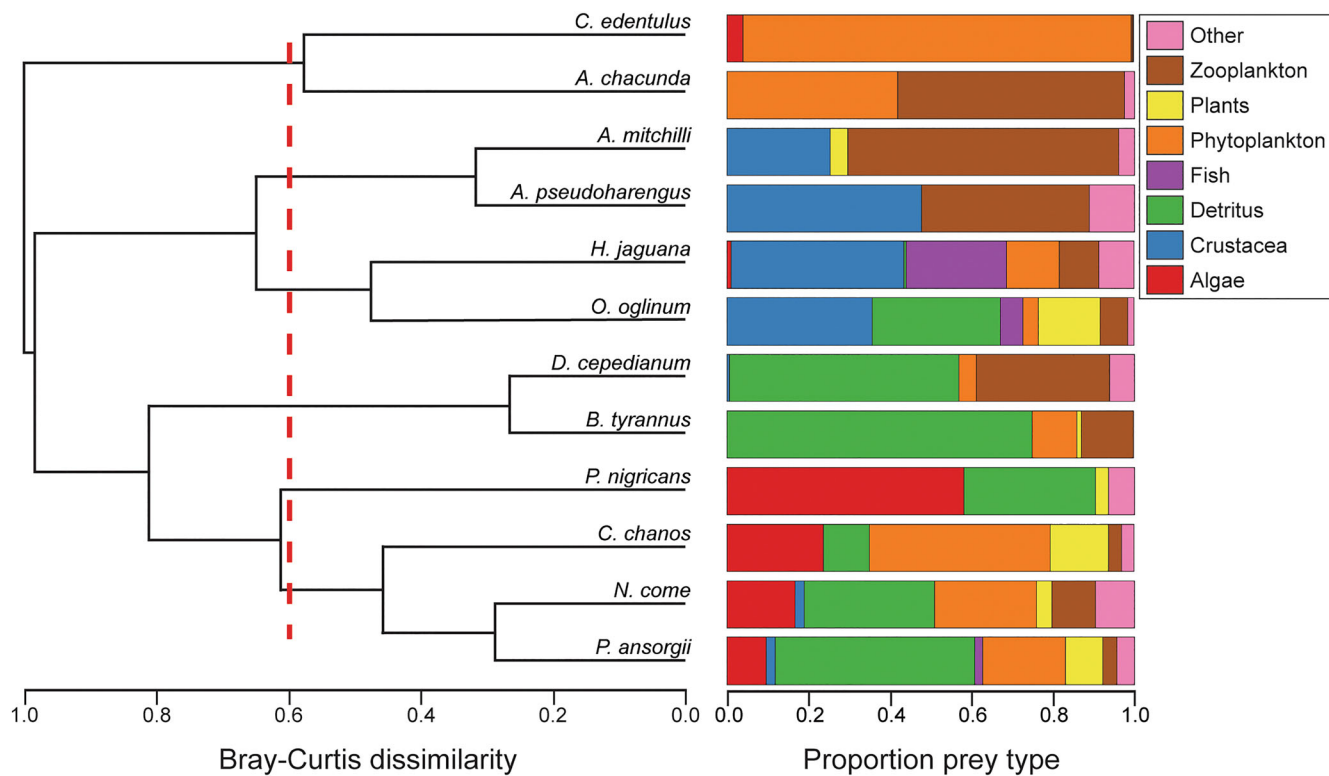


**FIGURE 8** Dendrogram resulting from hierarchical agglomerative clustering based on Bray–Curtis dissimilarity of prey type for 12 otomorphan species. The distance on the *x*-axis is representative of the similarity of any two species based on diet specialization. The dashed line indicates the critical dissimilarity value (0.6). Diet composition was taken from existing quantitative studies, and prey type was grouped into eight categories that comprise at least 1% of a species diet. Note the absence of *Tenualosa thibaudeau* for which quantitative dietary data did not exist.

for which we provide the first anatomical description of the EBO. We found that otomorphan EBOs, while phenotypically diverse and widely distributed throughout the clade, share numerous anatomical characteristics at both the gross and histological levels. We use these findings to (1) establish a new system for categorizing the anatomical diversity of EBOs, (2) assess the relationship between EBO anatomy, phylogeny, and diet, and (3) discuss existing hypotheses regarding the evolutionary origin of EBOs in Otomorpha.

#### 4.1 | A new system of categorization for EBO diversity

We have identified five axes of variation that describe diversity in morphology, tissue composition, and histological architecture of the EBO. These are (1) shape of the organ and diverticulum (i.e., round vs. elongate, coiled vs. not coiled), (2) size relative to the branchial basket, (3) gill raker morphology, (4) muscularity, and (5) adiposity. We posit that these five axes of variation are a more versatile and functionally informative means

of categorizing EBO diversity than what has previously been proposed. The most comprehensive and taxonomically extensive treatment of EBO diversity is Bertmar et al.'s (1969) synthesis of the literature, which included an original delineation of EBOs, each categorized into one of seven discrete types. By contrast, we describe the anatomical diversity of the EBO as a set of continuous traits. This allows for greater precision and more detailed descriptions of complex anatomy, providing what we believe is a better representation of variation. Additionally, Bertmar et al.'s types relied on phylogenies we now know to be erroneous at multiple taxonomic levels, most pertinently within Clupeiformes and in the nesting of characid fishes within Cypriniformes (Bloom & Lovejoy, 2012; Egan et al., 2018; Egan et al., 2024; Fink & Fink, 1981; Greenwood et al., 1966; Lavoué et al., 2013; Whitehead, 1962). This renders the descriptions of some types (i.e., remnant, vestigial tube, primitive expanded sac, derivative expanded sac) phylogenetically inaccurate and functionally uninformative. Finally, our study includes histological data, allowing for a comparison of EBO morphology at the tissue/cellular level, which can

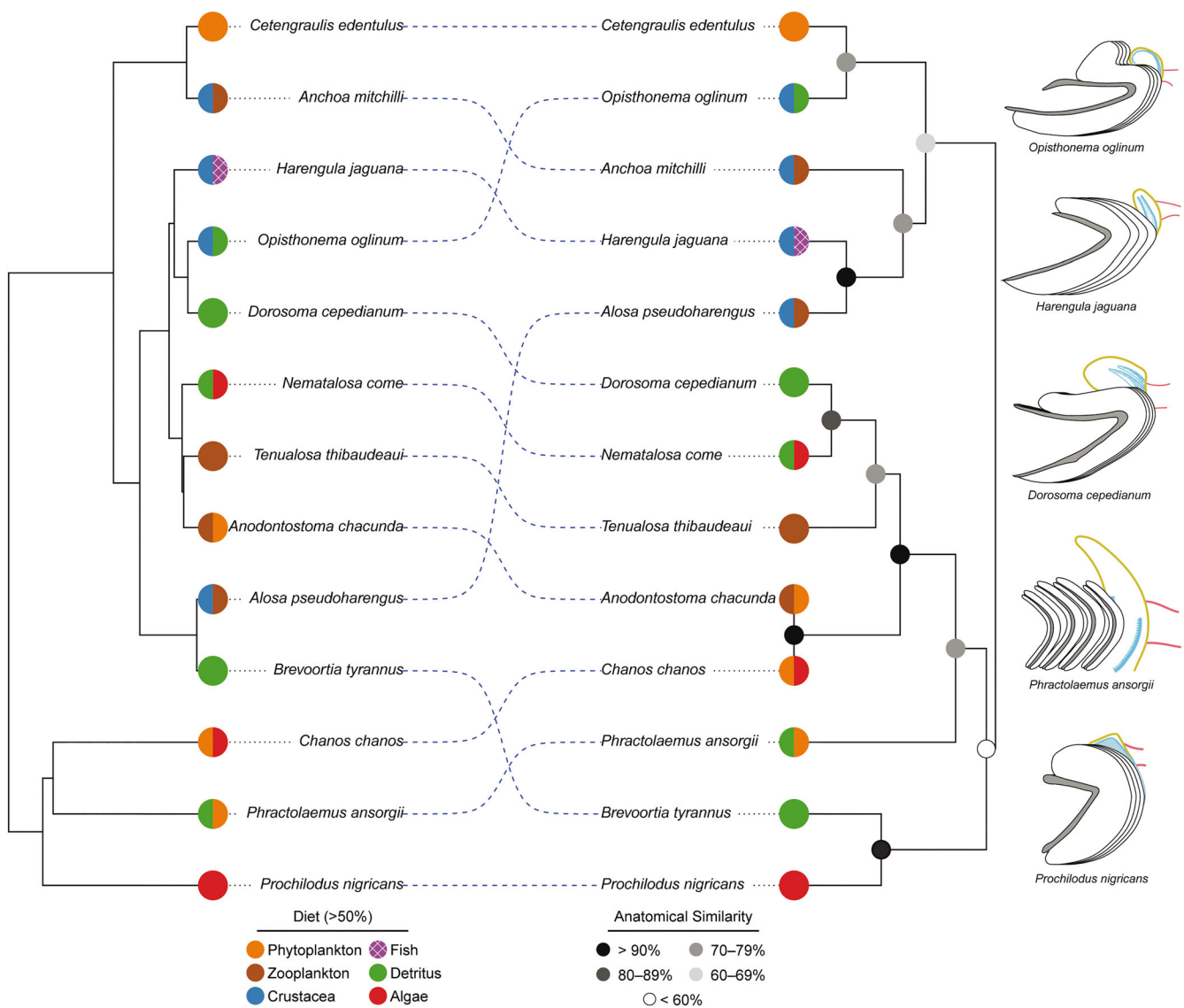


**FIGURE 9** Tanglegram of evolutionary relatedness (left) and anatomical similarity (right) of EBOs. Diet mapped onto phylogeny with colored circles representing the major prey groups that constitute 50% or more of the diet (two colors denotes the two prey types that together constitute over 50% of diet.; see Figure 8) Note the inclusion of *Tenualosa thibaudeaui*, for which only qualitative observation of diet has been reported (Rainboth, 1996; Vidhayanon, 2005). Anatomical similarity of EBOs is based on the presence/absence of discrete anatomical traits (Table 2). Percentages reported are the approximately unbiased *p*-values of each node.

better inform functional hypotheses for how the EBO may be used in feeding.

For example, our histological findings reveal that several EBOs (*A. mitchilli*, *A. pseudoharengus*) previously described as vestigial or small remnants are actually highly muscular structures, richly papillated, and lined by an epithelium studded with mucus-producing cells (Figure 5a,b). Maintaining musculature and producing glycoproteins is energetically costly (Bansil & Turner, 2018; McShane et al., 2021), making it unlikely that these EBOs are functionally obsolete or “degenerate.” Instead, their distinct morphologies may reflect adaptations driven by diet, historical contingency, or specific EBO

functions. *A. mitchilli*, as an example, primarily consumes larger prey (zooplankton and small crustaceans) than many of the other species included in our study (Livingston, 1982). Some of these prey items are too large to fit inside the EBO, suggesting that the diverticula do not function as the site of food aggregation but rather primarily as a structure for mucus secretion. In light of new phylogenetic and ecological data, our study of previously described EBOs has revealed anatomical complexity that may have functional correlates in feeding.

Our findings and axes of morphological variation have functional implications for how the EBO aggregates small, low-nutrient food items and expels them in a

concentration suitable for consumption (Bertmar et al., 1969; Kapoor, 1957; Miller, 1864). Size and shape of the organ may place a limit on how much food can be aggregated as well as how large these food particles can be. Epithelial structures like papillae and the mucus-producing cells that line them likely affect how food particles aggregate and are transported into and out of the diverticulum. Long papillae, such as those found in the terminus of *C. chanos* (Figure 7*i*), may aid in keeping food trapped or directing food into the blind end of the diverticulum (Mahdy et al., 2021), whereas muscularly invested papillae may supply some degree of internal hydrodynamic control to move particle-laden fluid through the diverticulum. Many studies have documented the integral role of mucus in the mechanical capture, aggregation, and transport of food particles during and after the filtration process (Hoogenboezem & Boogaart, 1993; Sanderson et al., 1996; Sanderson & Wassersug, 1993; Ward et al., 1993). The presence of goblet cells has been recorded in the EBOs of many species, and the secreted mucus has been suggested to aid in the entrapment of food as it increases the viscosity of fluid in the EBO, facilitating the formation of boli (Cohen & Hernandez, 2018; Cone, 2009; Hansen et al., 2014; Holley et al., 2015; Miller, 1964).

Muscularity and adiposity of the organ are also important functional components, given that in addition to being concentrated, food must be expelled for consumption. The degree of muscularity may be indicative of the capacity for compressive force, which would be especially relevant for long, coiling EBOs in which food is packed tightly all the way to the terminus of the diverticulum (Figures 1*b* and 4*c–g*). Long, coiling EBOs also have the most adipose tissue, a correlation that may relate to their ability to withstand strain and prolonged pressure during compression; additionally, adipose tissue may help maintain three-dimensional volume and contribute to turgidity while the EBO fills with food and fluid (Guimarães et al., 2020; Kuhns, 1949; Miller-Young et al., 2002). Many EBOs possess an abundance of both fat and muscle (Table 2), suggesting that they are critical components of efficient feeding on microscopic prey; further study could determine the biomechanical properties of these traits as well as any functional significance of their variation in the role of aggregation and feeding. It is natural then to question how strongly prey type correlates with anatomical variation or whether patterns of morphological diversity are conserved among closely related species.

## 4.2 | Anatomy–phylogeny and anatomy–diet correlations

We proposed two alternative hypotheses to explain the evolution and functional significance of EBO diversity

(1) that variation in EBO anatomy could be best explained by phylogenetic relatedness and (2) that variation in EBO anatomy could be best explained by diet. Our results, however, suggest that neither hypothesis completely explains the morphological variation of otomorphan EBOs.

There are instances of closely related species possessing anatomically similar EBOs, but there are also instances of distantly related species possessing anatomically similar EBOs. For example, *N. come*, *A. chacunda*, and *T. thibaudeau* are closely related lineages of clupeiform. These species possess EBOs that are round and thickly walled, adipose-rich, with coiling diverticula (Figure 4*c,f,g*). Their diets overlap in some prey categories, namely, zooplankton and phytoplankton, which are present in different proportions (Figure 8). *N. come*'s diet is the most varied, composed primarily of detritus (32%), algae (25%), phytoplankton (16.7%), and zooplankton (10.7%). *A. chacunda*'s diet is mostly composed of zooplankton (55.6%) and phytoplankton (41.9%), and *T. thibaudeau*, for which there is no quantitative dietary data, has been reported to feed on zooplankton (Rainboth, 1966; Vidthayanon, 2005) (Table 3). However, distantly related species such as *C. chanos* and *D. cepedianum* also possess round, adipose-rich, coiling EBOs (Figure 4*d,e*) despite feeding on a different composition of prey items; this contradicts both our hypotheses. The anatomical resemblance of some of these EBOs in the face of millions of years of evolutionary distance is particularly striking (Figure 2*b*) (Betancur-R et al., 2017; Egan et al., 2024). *A. chacunda*, a clupeiform, scored identically to *C. chanos*, a gonorynchiform, in our anatomical character matrix. Both of these species feed on phytoplankton and zooplankton, though detritus, algae, and plants constitute a large proportion of the diet of *C. chanos* as well (Figure 8 and Table 3).

It is not the case, however, that all species feeding on similar prey possess anatomically similar EBOs. For example, *Cetengraulis edentulus*, a clupeiform that, like all aforementioned species, feeds on phytoplankton, possesses a round, sac-like EBO with thin but muscular walls possessing very little adipose tissue. In fact, the EBO of *C. edentulus* more closely resembles those of species that feed on crustaceans, which are characterized by muscularly invested papillae and thinner walls composed of muscle with little to no adipose tissue (Figure 9). Another example of morphological variation in fish feeding on similar diets can be seen in the detritivorous *D. cepedianum* and *B. tyrannus*, the two species that consume the most similar diets within our study (Figure 8). Both species are clupeiforms, though they belong to different clades that diverged from a common ancestor >75 ma (Egan et al., 2018; Egan et al., 2024), and they differ dramatically on nearly every axis of morphological

variation (Figures 4d and 5e). Furthermore, *Phractolaemus ansorgii*, another species that feeds largely on detritus, possesses an EBO that is elongate, narrow, and morphologically distinct from that of all other detritivores (Figure 5d).

It is possible that a given EBO morphology evolved to be best at aggregating one type of food in an ancestral lineage, but because it was sufficiently able to aggregate other prey, it was retained during dietary shifts throughout evolution. It is also possible that certain aspects of diet may have resulted in convergent evolution, but with our present data, it is difficult to determine which prey types or aspects of trophic ecology have the strongest effects on EBO anatomy and which may be obscuring existing patterns. Future studies that incorporate a larger taxonomic sampling could further elucidate any correlations between anatomy, phylogeny, and diet.

We offer an alternative hypothesis to explain EBO diversity—that the complex interaction of historical contingency, morphological constraint, and other selective pressures, like feeding mode, are more significant factors in explaining EBO anatomy. Feeding mode is an aspect of feeding ecology that we did not consider in this study, although variation exists within our sample. For example, *D. cepedianum* and *B. tyrannus* both consume large quantities of detritus and zooplankton. However, *D. cepedianum* consumes small particles via intermittent suction suspension feeding, while *B. tyrannus* accomplishes this through continuous ram suspension feeding (Durbin & Durbin, 1975; Friedland et al., 1984; Miller, 1960; Sanderson & Wassersug, 1993). It is possible that these different feeding modes are associated with unique selective pressures that resulted in the evolution of distinct EBO morphologies. However, this idea requires further exploration because functional feeding differences (e.g., hydrodynamic forces in the oropharyngeal cavity during feeding and prey capture rates) between these species remain unknown. Additionally, the function of the EBO may be more varied than previously believed. Some species, like *A. mitchilli*, that are feeding on prey larger than the opening of the diverticulum of their EBO may not use their EBO as a site for food aggregation and may have co-opted this mucus-producing organ for yet another undescribed function, further obfuscating the role of diet in EBO morphology.

#### 4.3 | Evolutionary origins of the epibranchial organ

Epibranchial organ evolution has not been studied with any rigorous comparative methods, and a consensus on whether EBOs are convergent or homologous structures

has not been definitively reached. Nelson (1967), in a descriptive study of epibranchial bone anatomy, posited that EBOs evolved independently in each of the otomorphan lineages in which they occur. Furthermore, he suggested that these structures evolved from an ancestor with a more generalized branchial anatomy in response to repeated adoption of microphagous feeding tendencies. In contrast, Bertmar et al. (1969) stated that the striking morphological similarity among EBOs is unlikely to be a product of convergence, and all incidences of epibranchial organs are instead derived from a single origin within a common ancestral group, such as pholidophoroid holosteans.

We find the argument for homology intriguing, though insufficient in accounting for such a mottled distribution of EBOs across Otomorpha, as it would require significant character loss and reacquisition to explain why most otomorphans do not have an EBO. Of the over 4000 species of extant cypriniforms, EBOs have been described in only two members of the genus *Hypophthalmichthys* (*H. molitrix* and *H. nobilis*) (Boulenger, 1901; Cohen et al., 2020; Cohen & Hernandez, 2018; Hansen et al., 2014). Even within Clupeiformes, the group in which taxonomic diversity of EBOs is the highest, EBOs are not ubiquitous across the order. Epibranchial organs have been documented in 24 of 82 clupeiform genera (pers. comm., Joshua Egan), again suggesting significant loss and reacquisition should the plesiomorphic condition be to possess an EBO.

Instead of all EBOs being homologous structures, Nelson (1967) proposed that the homologous trait is not the EBO itself but rather the potentiality to evolve one. We find this argument to be better supported by our current understanding of otomorphan relationships and recent work on EBO development. We hypothesize that EBOs are not convergent structures evolved de novo in every otomorphan order; rather, EBOs are a form of biological atavism, a re-evolution of an ancestral trait no longer present phenotypically but lying dormant in the genome (Hall, 1984; Tomić & Meyer-Rochow, 2011). A study by Cohen et al. (2022) put forth a similar hypothesis that across Otomorpha, EBOs are developmentally homologous but may be functionally convergent in many instances. This hypothesis is informed by developmental data collected on three species—*Anchoa mitchilli* (clupeiform), *Brevoortia tyrannus* (clupeiform), *Hypophthalmichthys molitrix* (cypriniform)—with EBOs of wildly different morphological complexity. Cohen et al. (2022) showed that EBOs develop remarkably similarly, beginning as an involution of epithelial cells in the pharyngeal skeletal muscle above the fourth branchial arch. Our findings are consistent with those of prior studies in that EBOs are made up of the same basic components.

We suggest that the origin of EBOs is a matter of deep homology, an example of morphological diversification that utilizes the same fundamental building blocks to achieve a common goal—that of aggregating food. In congruence with Nelson (1967), we suggest that the ancestor of Otomorphan fishes did not necessarily have an EBO but rather the capacity to evolve one, and subsequent clades evolved EBOs in parallel as a response to shifts toward a microphagous diet. The specific resulting EBO morphologies may have been a product of feeding behavior or the series of idiosyncratic events in the species evolutionary history or simply a matter of building whatever structural properties permitted them to aggregate small particles well enough to survive.

However, to ascribe such a complex yet widespread adaptation to the serendipity of evolution alone would be to downplay the otomorphan potential for morphological novelty. Adaptations of the pharynx are common among otomorphans and represent a previously neglected axis of diversity that is a critical component of feeding biology. In addition to EBOs, pharyngeal structures include the palatal organ found in nearly all cypriniforms, the crumenal organs of alepocephaliforms, and the labyrinthine organ and suprabranchial chamber of air-breathing siluriforms (Boulenger, 1901; Cohen & Hernandez, 2018; Doosey & Bart Jr., 2011; Greenwood & Rosen, 1971; Hernandez & Cohen, 2019; Hughes & Munshi, 1973; Maina & Maloiy, 1986; Singh & Hughes, 1971). In fact, all but the gymnotiforms have evolved at least one organ in the posterior pharynx. Indeed, otomorphans exhibit an incredible propensity to build soft-tissued, often muscular structures in the pharynx, and one must wonder why this region within this clade provides such a rich substrate for complex and multidimensional morphological diversity.

## ACKNOWLEDGMENTS

The authors thank the following museums for the use of specimens: American Museum of Natural History (AMNH), James Ford Bell Museum of Natural History (JFBM), The Field Museum (FMNH), Texas A&M University Biodiversity Research and Teaching Collections (TCWC), Royal Ontario Museum (ROM), and the Virginia Institute of Marine Science (VIMS).

## FUNDING INFORMATION

A. J. E. was funded by the George Washington University Wilbur V. Harlan Research Fellowship and an NSF Graduate Research Fellowship [DGE-1746914]. J. M. H. was funded by an NSF Graduate Research Fellowship [DGE-1746914].

## ORCID

- Allyson J. Evans  <https://orcid.org/0009-0000-6851-2780>  
L. Patricia Hernandez  <https://orcid.org/0000-0001-9616-7777>

## REFERENCES

- Almeida, A., Behr, E., & Baldisserotto, B. (2013). Gill rakers in six teleost species: Influence of feeding habit and body size. *Ciencia Rural*, 43(12), 2208–2214.
- Arratia, G. (2018). Otomorphs (= otocephalans or ostarioclupemorphs) revisited. *Neotropical Ichthyology*, 16, e180079.
- Bansil, R., & Turner, B. S. (2018). The biology of mucus: Composition, synthesis and organization. *Advanced Drug Delivery Reviews*, 124, 3–15.
- Bauchot, R., Ridet, J. M., & Diagne, M. (1993). The epibranchial organ, its innervation and its probable functioning in *Heterotis niloticus* (Pisces, Teleostei, Osteoglossidae). *Environmental Biology of Fishes*, 37, 307–315.
- Bensam, P. (1964). The pharyngeal pockets in the Indian oil sardine, *Sardinella longiceps* Valenciennes and a few other clupeiformes from Indian waters. *Indian Journal Of Fisheries*, 11(1), 175–180.
- Bertmar, G., Kapoor, B., & Miller, R. V. (1969). Epibranchial organs in lower Teleostean fishes—An example of structural adaptation. *Review of General and Experimental Zoology*, 4, 1–48.
- Bertmar, G., & Strömberg, C. (1969). The feeding mechanisms in plankton eaters: I. The epibranchial organs in whitefish. *Marine Biology*, 3, 107–109.
- Betancur-R, R., Wiley, E. O., Arratia, G., Acero, A., Bailly, N., Miya, M., Lecointre, G., & Ortí, G. (2017). Phylogenetic classification of bony fishes. *BMC Evolutionary Biology*, 17, 1–40.
- Bloom, D. D., & Lovejoy, N. (2012). Molecular phylogenetics reveals a pattern of biome conservatism in New World anchovies (family Engraulidae). *Journal of Evolutionary Biology*, 25(4), 701–715.
- Boulenger, G. A. (1901). XXV—On the presence of a superbranchial organ in the cyprinoid fish *Hypophthalmichthys*. *Journal of Natural History*, 8(45), 186–188.
- Bray, J. R., & Curtis, J. T. (1957). An ordination of the upland forest communities of southern Wisconsin. *Ecological Monographs*, 27(4), 326–349.
- Brodnick, O. B., Hansen, C. E., Huie, J. M., Brandl, S. J., & Worsaae, K. (2022). Functional impact and trophic morphology of small, sand-sifting fishes on coral reefs. *Functional Ecology*, 36, 1936–1948. <https://doi.org/10.1111/1365-2435.14087>
- Buchheister, A., & Latour, R. J. (2015). Diets and trophic-guild structure of a diverse fish assemblage in Chesapeake Bay, USA. *Journal of Fish Biology*, 86(3), 967–992.
- Camp, A. L., Roberts, T. J., & Brainerd, E. L. (2015). Swimming muscles power suction feeding in largemouth bass. *Proceedings of the National Academy of Sciences*, 112(28), 8690–8695.
- Capanna, E., Cataudella, S., & Monaco, G. (1974). The pharyngeal structure of mediterranean mugilidae. *Monitore Zoologico Italiano-Italian Journal of Zoology*, 8(1–2), 29–46.
- Carr, W. E., & Adams, C. A. (1973). Food habits of juvenile marine fishes occupying seagrass beds in the estuarine zone near Crystal River, Florida. *Transactions of the American Fisheries Society*, 102(3), 511–540.

- Cohen, K. E., Ackles, A. L., & Hernandez, L. P. (2022). The role of heterotopy and heterochrony during morphological diversification of otocephalan epibranchial organs. *Evolution & Development*, 24(3–4), 79–91.
- Cohen, K. E., George, A. E., Chapman, D. C., Chick, J. H., & Hernandez, L. P. (2020). Developmental ecomorphology of the epibranchial organ of the silver carp, *Hypophthalmichthys molitrix*. *Journal of Fish Biology*, 97(2), 527–536.
- Cohen, K. E., & Hernandez, L. P. (2018). The complex trophic anatomy of silver carp, *Hypophthalmichthys molitrix*, highlighting a novel type of epibranchial organ. *Journal of Morphology*, 279(11), 1615–1628.
- Cohen, K. E., Lucanus, O., Summers, A. P., & Kolmann, M. A. (2023). Lip service: Histological phenotypes correlate with diet and feeding ecology in herbivorous pacus. *The Anatomical Record*, 306(2), 326–342.
- Cone, R. A. (2009). Barrier properties of mucus. *Advanced Drug Delivery Reviews*, 61(2), 75–85.
- D'Aubenton, F. (1955). Étude de l'appareil branchiospinal et de l'organe suprabranchial de *Heterotis niloticus*. *Bulletin de l'Institut fondamental d'Afrique noire*, 17(4), 1179–1201.
- Doosey, M. H., & Bart, H. L., Jr. (2011). Morphological variation of the palatal organ and chewing pad of Catostomidae (Teleostei: Cypriniformes). *Journal of Morphology*, 272(9), 1092–1108.
- Durbin, A. D., Durbin, E. G., Verity, P. G., & Sinayda, T. J. (1981). Voluntary swimming speeds and respiration rates of a filter feeding planktivore, the Atlantic menhaden, *Brevoortia tyrannus* (Pisces: Clupeidae). *Fishery Bulletin*, 78, 877.
- Durbin, A. G., & Durbin, E. G. (1975). Grazing rates of the Atlantic menhaden *Brevoortia tyrannus* as a function of particle size and concentration. *Marine Biology*, 33(3), 265–277.
- Egan, J. P., Bloom, D. D., Kuo, C. H., Hammer, M. P., Tongnunui, P., Iglesias, S. P., Sheaves, M., Grudpan, C., & Simons, A. M. (2018). Phylogenetic analysis of trophic niche evolution reveals a latitudinal herbivory gradient in *Clupeoidei* (herrings, anchovies, and allies). *Molecular Phylogenetics and Evolution*, 124, 151–161.
- Egan, J. P., Chew, U. S., Kuo, C. H., Villarroel-Diaz, V., Hundt, P. J., Iwinski, N. G., Hammer, M. P., & Simons, A. M. (2017). Diets and trophic guilds of small fishes from coastal marine habitats in western Taiwan. *Journal of Fish Biology*, 91(1), 331–345.
- Egan, J. P., Simons, A. M., Alavi-Yeganeh, M. S., Hammer, M. P., Tongnunui, P., Arcila, D., Betancur-R, R., & Bloom, D. D. (2024). Phylogenomics, lineage diversification rates, and the evolution of diadromy in Clupeiformes (anchovies, herrings, sardines, and relatives). *Systematic Biology*, 73(4), 683–703.
- Ewers, L. A., & Boesel, M. W. (1935). The food of some Buckeye Lake fishes. *Transactions of the American Fisheries Society*, 65(1), 57–70.
- Fink, S. V., & Fink, W. L. (1981). Interrelationships of the ostariophysan fishes (Teleostei). *Zoological Journal of the Linnean Society*, 72(4), 297–353.
- Forey, P. L. (1975). A fossil clupeomorph fish from the Albian of the Northwest Territories of Canada, with notes on cladistic relationships of clupeomorphs. *Journal of Zoology*, 175(2), 151–177.
- Friedland, K. (1985). Functional morphology of the branchial basket structures associated with feeding in the Atlantic menhaden, *Brevoortia tyrannus* (Pisces: Clupeidae). *Copeia*, 4, 1018–1027.
- Friedland, K. D., Haas, L. W., & Merriner, J. V. (1984). Filtering rates of the juvenile Atlantic menhaden *Brevoortia tyrannus* (Pisces: Clupeidae), with consideration of the effects of detritus and swimming speed. *Marine Biology*, 84, 109–117.
- Gay, D., Bassani, C., & Sergipense, S. (2002). Diel variation and selectivity in the diet of *Cetengraulis edentulus* (Cuvier 1828) (Engraulidae-Clupeiformes) in the Itaipu Lagoon, Niterói, Rio de Janeiro. *Atlântica, Rio Grande*, 24(2), 59–68.
- Greenwood, P. H., & Rosen, D. E. (1971). Notes on the structure and relationships of the alepocephaloid fishes. *American Museum Novitates*; no. 2473.
- Greenwood, P. H., Rosen, D. E., Weitzman, S. H., & Myers, G. S. (1966). Phyletic studies of teleostean fishes, with a provisional classification of living forms. *Bulletin of the American Museum of Natural History*, 131, 339–446.
- Guimarães, C. F., Gasperini, L., Marques, A. P., & Reis, R. L. (2020). The stiffness of living tissues and its implications for tissue engineering. *Nature Reviews Materials*, 5, 351–370. <https://doi.org/10.1038/s41578-019-0169-1>
- Hall, B. K. (1984). Developmental mechanisms underlying the formation of atavisms. *Biological Reviews*, 59(1), 89–122.
- Hansen, A., Ghosal, R., Caprio, J., Claus, A. W., & Sorensen, P. W. (2014). Anatomical and physiological studies of bigheaded carps demonstrate that the epibranchial organ functions as a pharyngeal taste organ. *Journal of Experimental Biology*, 217(21), 3945–3954.
- Heim, W. (1935). Über die Rachensäcke der Characidae und über verwandte akzessorische Organe bei andern Teleosteern. *Zoologische Jahrbücher. Abteilung für Anatomie und Ontogenie der Tiere*, 60, 61–106.
- Heiple, Z., Huie, J. M., Medeiros, A. P. M., Hart, P. B., Goatley, C. H. R., Arcila, D., & Miller, E. C. (2023). Many ways to build an angler: Diversity of feeding morphologies in a deep-sea evolutionary radiation. *Biology Letters*, 19, 20230049. <https://doi.org/10.1098/rsbl.2023.0049>
- Hernandez, L. P., & Cohen, K. E. (2019). The role of developmental integration and historical contingency in the origin and evolution of cypriniform trophic novelties. *Integrative and Comparative Biology*, 59(2), 473–488.
- Hiatt, R. W. (1947). Food-chains and the food cycle in Hawaiian fish ponds—part I. The food and feeding habits of mullet (*Mugil cephalus*), milkfish (*Chanos chanos*), and the ten-pounder (*Elops macrurus*). *Transactions of the American Fisheries Society*, 74(1), 250–261.
- Holley, L. L., Heidman, M. K., Chambers, R. M., & Sanderson, S. L. (2015). Mucous contribution to gut nutrient content in American gizzard shad *Dorosoma cepedianum*. *Journal of Fish Biology*, 86(5), 1457–1470.
- Hoogenboezem, W., & Boogaart, J. G. M. (1993). Importance of mucus in filter-feeding of bream (*Abramis brama*). *Canadian Journal of Fisheries and Aquatic Sciences*, 50, 472–479.
- Horinouchi, M., & Sano, M. (2000). Food habits of fishes in a Zosteraria marina bed at Aburatsubo, central Japan. *Ichthyological Research*, 47, 163–173.
- Horinouchi, M., Tongnunui, P., Furumitsu, K., Nakamura, Y., Kanou, K., Yamaguchi, A., Okamoto, K., & Sano, M. (2012).

- Food habits of small fishes in seagrass habitats in Trang, southern Thailand. *Fisheries Science*, 78, 577–587.
- Hughes, G. M., & Munshi, J. D. (1973). Nature of the air-breathing organs of the Indian fishes *Channa*, *Amphipnous*, *Clarias* and *Saccobranchus* as shown by electron microscopy. *Journal of Zoology*, 170(2), 245–270.
- Huie, J. M., Thacker, C. E., & Tornabene, L. (2020). Co-evolution of cleaning and feeding morphology in western Atlantic and eastern Pacific gobies. *Evolution*, 74(2), 419–433. <https://doi.org/10.1111/evo.13904>
- Hundt, P. J., Nakamura, Y., & Yamaoka, K. (2014). Diet of combtooth blennies (Blenniidae) in Kochi and Okinawa, Japan. *Ichthyological Research*, 61, 76–82.
- Hundt, P. J., & Simons, A. M. (2018). Extreme dentition does not prevent diet and tooth diversification within combtooth blennies (Ovalentaria: Blenniidae). *Evolution*, 72(4), 930–943.
- Inoue, T., Yusuke, S., & Sano, M. (2005). Food habits of fishes in the surf zone of a sandy beach at Sanrimatsubara, Fukuoka prefecture, Japan. *Ichthyological Research*, 52, 9–14.
- Iwai, I. (1956). The anatomy of the pharyngeal pockets of the Japanese gizzard shad, *Kynosurus punctatus* (Temminck & Schlegel). *Bulletin Japanese Society of Scientific Fisheries*, 22, 9–11.
- Jude, D. J. (1973). Food and feeding habits of gizzard shad in Pool 19, Mississippi River. *Transactions of the American Fisheries Society*, 102(2), 378–383.
- Kahane-Rapport, S. R., & Paig-Tran, E. W. M. (2024). Suspension feeding in fishes. In S. L. Alderman & T. E. Gillis (Eds.), *Encyclopedia of fish physiology* (2nd ed., pp. 519–534). Academic Press. <https://doi.org/10.1016/B978-0-323-90801-6.00078-1>
- Kapoor, B. G. (1954). The pharyngeal organ and its associated structures in the milk-fish, *Chanos chanos* (Forskål). *Journal of the Zoological Society of India*, 6, 51–58.
- Kohler, C. C., & Ney, J. J. (1980). Piscivory in a land-locked alewife (*Alosa pseudoharengus*) population. *Canadian Journal of Fisheries and Aquatic Sciences*, 37(8), 1314–1317.
- Kolmann, M. A., Hughes, L. C., Hernandez, L. P., Arcila, D., Betancur-R, R., Sabaj, M. H., López-Fernández, H., & Ortí, G. (2021). Phylogenomics of piranhas and pacus (Serrasalmidae) uncovers how dietary convergence and parallelism obfuscate traditional morphological taxonomy. *Systematic Biology*, 70(3), 576–592.
- Kolmann, M. A., Huie, J. M., Evans, K., & Summers, A. P. (2018). Specialized specialists and the narrow niche fallacy: A tale of scale-feeding fishes. *Royal Society Open Science*, 5(1), 171581. <https://doi.org/10.1098/rsos.171581>
- Kuhns, J. G. (1949). Changes in elastic adipose tissue. *Journal of Bone and Joint Surgery*, 31(3), 541–547.
- Kutkuhn, J. H. (1958). Utilization of plankton by juvenile gizzard shad in a shallow prairie lake. *Transactions of the American Fisheries Society*, 87(1), 80–103.
- Lavoué, S., Miya, M., Musikasinthorn, P., Chen, W. J., & Nishida, M. (2013). Mitogenomic evidence for an Indo-west Pacific origin of the Clupeoidei (Teleostei: Clupeiformes). *PLoS One*, 8(2), e56485.
- Legendre, P., & Legendre, L. (2012). *Numerical ecology* (Vol. 24). Elsevier.
- Lewis, V. P., & Peters, D. S. (1994). Diet of juvenile and adult Atlantic menhaden in estuarine and coastal habitats. *Transactions of the American Fisheries Society*, 123(5), 803–810.
- Livingston, R. J. (1982). Trophic organization of fishes in a coastal seagrass system. *Marine Ecology Progress Series*, 7(1), 1–12.
- Mahdy, M. A., Abdalla, K. E., & Mohamed, S. A. (2021). Morphological and scanning electron microscopic studies of the lingual papillae of the tongue of the goat (*Capra hircus*). *Microscopy Research and Technique*, 84(5), 891–901.
- Maina, J. N., & Maloiy, G. M. O. (1986). The morphology of the respiratory organs of the African air-breathing catfish (*Clarias mossambicus*): A light, electron and scanning microscopic study, with morphometric observations. *Journal of Zoology*, 209(3), 421–445.
- McShane, A., Bath, J., Jaramillo, A. M., Ridley, C., Walsh, A. A., Evans, C. M., Thornton, D. J., & Ribbeck, K. (2021). Mucus. *Current Biology*, 31(15), R938–R945.
- Miller, R. R. (1960). Systematics and biology of the gizzard shad (*Dorosoma cepedianum*) and related fishes. *Fisheries*, 1(2), 3.
- Miller, R. V. (1964). The morphology and function of the pharyngeal organs in the clupeid, *Dorosoma petenense* (Günther). *Chesapeake Science*, 5, 194–199.
- Miller, R. V. (1969). Constancy of epibranchial organs and fourth epibranchial bones within species groups of clupeid fishes constancy of epibranchial organs and fourth epibranchial bones within species groups of clupeid fishes. *Copeia*, 2, 308–312.
- Miller-Young, J. E., Duncan, N. A., & Baroud, G. (2002). Material properties of the human calcaneal fat pad in compression: Experiment and theory. *Journal of Biomechanics*, 35(12), 1523–1531.
- Modde, T., & Ross, S. T. (1983). Trophic relationships of fishes occurring within a surf zone habitat in the northern Gulf of Mexico. *Gulf of Mexico Science*, 6(2), 4.
- Nakamura, Y., Horinouchi, M., Nakai, T., & Sano, M. (2003). Food habits of fishes in a seagrass bed on a fringing coral reef at Iriomote Island, southern Japan. *Ichthyological Research*, 50, 15–22.
- Nanjo, K., Kohno, H., & Sano, M. (2008). Food habits of fishes in the mangrove estuary of Urauchi River, Iriomote Island, southern Japan. *Fisheries Science*, 74, 1024–1033.
- Near, T. J., Dornburg, A., & Friedman, M. (2014). Phylogenetic relationships and timing of diversification in gonorynchiform fishes inferred using nuclear gene DNA sequences (Teleostei: Ostariophysi). *Molecular Phylogenetics and Evolution*, 80, 297–307.
- Nelson, G. J. (1967). Epibranchial organs in lower teleostean fishes. *Journal of Zoology*, 153, 71–89.
- Nelson, J. S., Grande, T. C., & Wilson, M. V. (2016). *Fishes of the world*. John Wiley & Sons.
- Odum, O., & Anuta, M. (2001). The food and feeding habits of *Phractolaemus anosrgii* (Boulenger) from Warri River, Nigeria. *Journal of Aquatic Sciences*, 16(1), 18–21.
- Odum, W. E., & Heald, E. J. (1972). Trophic analyses of an estuarine mangrove community. *Bulletin of Marine Science*, 22(3), 671–738.
- Oksanen, J., Blanchet, F. G., Kindt, R., Legendre, P., Minchin, P. R., O'hara, R. B., Simpson, G. L., Solymos, P., Stevens, M. H., & Wagner, H. (2013). Package ‘vegan’. *Community Ecology Package, Version*, 2(9), 1–295.
- Paig-Tran, M. E. W., & Summers, A. P. (2014). Comparison of the structure and composition of the branchial filters in suspension feeding elasmobranchs. *The Anatomical Record*, 297, 701–715. <https://doi.org/10.1002/ar.22850>

- Pasleau, F., Diogo, R., & Chardon, M. (2010). *The epibranchial organ and its anatomical environment in the Gonorynchiformes, with functional discussions. Gonorynchiformes and ostariophysan relationships: A comprehensive review* (pp. 145–171). Science Publishers.
- Pos, K. M., Farina, S. C., Kolmann, M. A., & Gidmark, N. J. (2019). Pharyngeal jaws converge by similar means, not to similar ends, when minnows (Cypriniformes: Leuciscidae) adapt to new dietary niches. *Integrative and Comparative Biology*, 59(2), 432–442.
- Pouilly, M., Yunoki, T., Rosales, C., & Torres, L. (2004). Trophic structure of fish assemblages from Mamoré River floodplain lakes (Bolivia). *Ecology of Freshwater Fish*, 13(4), 245–257.
- Rainboth, W. J. (1996). *Fishes of the Cambodian Mekong*. Food & Agriculture Organization.
- Revell, L. J. (2024). Phytools 2.0: An updated R ecosystem for phylogenetic comparative methods (and other things). *PeerJ*, 12, e16505. <https://doi.org/10.7717/peerj.16505>
- Roberts-Hughes, A. S., Martinez, C. M., Corn, K. A., & Wainwright, P. C. (2024). A classic key innovation constrains oral jaw functional diversification in fishes. *Evolution Letters*, 9(1), 24–40.
- Sanderson, S. L. (2024). Particle separation mechanisms in suspension-feeding fishes: Key questions and future directions. *Frontiers in Marine Science*, 11(1), 1331164.
- Sanderson, S. L., Cheer, A. Y., Goodrich, J. S., Graziano, J. D., & Callan, W. T. (2001). Crossflow filtration in suspension-feeding fishes. *Nature*, 412, 439–441. <https://doi.org/10.1038/35086574>
- Sanderson, S. L., Stebar, M. C., Ackermann, K. L., Jones, S. H., Batjakas, I. E., & Kaufman, L. (1996). Mucus entrapment of particles by a suspension-feeding tilapia (Pisces: Cichlidae). *Journal of Experimental Biology*, 199(8), 1743–1756.
- Sanderson, S. L., & Wassersug, R. (1993). Convergent and alternative designs for vertebrate suspension feeding. In J. Hanken & B. K. Hall (Eds.), *The skull: Functional and evolutionary mechanisms* (Vol. 3, pp. 37–112). University of Chicago Press.
- Schindelin, J., Arganda-Carreras, I., Frise, E., Kaynig, V., Longair, M., Pietzsch, T., Preibisch, S., Rueden, C., Saalfeld, S., Schmid, B., Tinevez, J. Y., White, D. J., Hartenstein, V., Eliceiri, K., Tomancak, P., & Cardona, A. (2012). Fiji: An open-source platform for biological-image analysis. *Nature Methods*, 9(7), 676–682. <https://doi.org/10.1038/nmeth.2019>
- Sims, D. W. (2000). Filter-feeding and cruising swimming speeds of basking sharks compared with optimal models: They filter-feed slower than predicted for their size. *Journal of Experimental Marine Biology and Ecology*, 249(1), 65–76.
- Singh, B. N., & Hughes, G. M. (1971). Respiration of an air-breathing catfish *Clarias batrachus* (Linn.). *Journal of Experimental Biology*, 55(2), 421–434.
- Soe, K. K., Pradit, S., & Hajisamae, S. (2021). Feeding habits and seasonal trophic guilds structuring fish community in the bay mouth region of a tropical estuarine habitat. *Journal of Fish Biology*, 99(4), 1430–1445.
- Stone, H. H., & Daborn, G. R. (1987). Diet of alewives, *Alosa pseudoharengus* and blueback herring, *A. aestivalis* (Pisces: Clupeidae) in Minas Basin, Nova Scotia, a turbid, macrotidal estuary. *Environmental Biology of Fishes*, 19, 55–67.
- Straube, N., Li, C., Mertzen, M., Yuan, H., & Moritz, T. (2018). A phylogenomic approach to reconstruct interrelationships of main clupeocephalan lineages with a critical discussion of morphological apomorphies. *BMC Evolutionary Biology*, 18, 1–17.
- Suzuki, R., & Shimodaira, H. (2006). Pvclust: An R package for assessing the uncertainty in hierarchical clustering. *Bioinformatics*, 22, 1540–1542.
- Takahasi, N. (1957). On the so-called accessory respiratory organ “gill-helix” found in some *Clupeiform* fishes, with special reference to its function and its genealogy. *Japanese Journal of Ichthyology*, 5(3–6), 71–77.
- Tomić, N., & Meyer-Rochow, V. B. (2011). Atavisms: Medical, genetic, and evolutionary implications. *Perspectives in Biology and Medicine*, 54(3), 332–353.
- Vega-Cendejas, M. E., Hernández, M., & Arreguin-Sánchez, F. (1994). Trophic interrelations in a beach seine fishery from the northwestern coast of the Yucatan peninsula, Mexico. *Journal of Fish Biology*, 44(4), 647–659.
- Vega-Cendejas, M. E., Mexicano-Cintora, G., & Arce, A. M. (1997). Biology of the thread herring *Opisthonema oglinum* (Pisces: Clupeidae) from a beach seine fishery of the Campeche Bank, Mexico. *Fisheries Research*, 30(1–2), 117–126.
- Vidthayanon, C. (2005). *Thailand red data: Fishes*. Office of Natural Resources and Environmental Policy and Planning.
- Ward, J. E., MacDonald, B. A., Thompson, R. J., & Beninger, P. G. (1993). Mechanisms of suspension feeding in bivalves: Resolution of current controversies by means of endoscopy. *Limnology and Oceanography*, 38(2), 265–272.
- Weller, H. I., McMahan, C. D., & Westneat, M. W. (2017). Dirt-sifting devilfish: Winnowing in the geophagine cichlid *Satanoperca daemon* and evolutionary implications. *Zoomorphology*, 136, 45–59.
- Whitehead, P. J. P. (1962). A contribution to the classification of clupeoid fishes. *Journal of Natural History*, 5(60), 737–750.

**How to cite this article:** Evans, A. J., Egan, J. P., Huie, J. M., & Hernandez, L. P. (2025). Comparative anatomy of otomorphan epibranchial organs. *The Anatomical Record*, 1–23. <https://doi.org/10.1002/ar.25663>